LETTER

doi:10.1038/nature16960

Vast assembly of vocal marine mammals from diverse species on fish spawning ground

Delin Wang[1], Heriberto Garcia[1], Wei Huang[1], Duong D. Tran[1], Ankita D. Jain[2], Dong Hoon Yi[2], Zheng Gong[1,2], J. Michael Jech[3], Olav Rune Godø[4], Nicholas C. Makris[2] & Purnima Ratilal[1]

Observing marine mammal (MM) populations continuously in time and space over the immense ocean areas they inhabit is challenging but essential for gathering an unambiguous record of their distribution, as well as understanding their behaviour and interaction with prey species[1–6]. Here we use passive ocean acoustic waveguide remote sensing (POAWRS)[7,8] in an important North Atlantic feeding ground[9,10] to instantaneously detect, localize and classify MM vocalizations from diverse species over an approximately 100,000 km^2 region. More than eight species of vocal MMs are found to spatially converge on fish spawning areas containing massive densely populated herring shoals at night-time[11–16] and diffuse herring distributions during daytime. We find the vocal MMs divide the enormous fish prey field into species-specific foraging areas with varying degrees of spatial overlap, maintained for at least two weeks of the herring spawning period. The recorded vocalization rates are diel (24 h)-dependent for all MM species, with some significantly more vocal at night and others more vocal during the day. The four key baleen whale species of the region: fin, humpback, blue and minke have vocalization rate trends that are highly correlated to trends in fish shoaling density and to each other over the diel cycle. These results reveal the temporospatial dynamics of combined multi-species MM foraging activities in the vicinity of an extensive fish prey field that forms a massive ecological hotspot, and would be unattainable with conventional methodologies. Understanding MM behaviour and distributions is essential for management of marine ecosystems and for accessing anthropogenic impacts on these protected marine species[1–5,17,18].

Here we present the ecosystem-wide spatial distributions of vocal MMs from multiple cetacean species, including both mysticetes and odontocetes, acquired simultaneously with that of their fish prey during their feeding season in the Gulf of Maine (GOM), an important North Atlantic MM foraging ground[9,10] (Figs 1 and 2). The GOM is among the more diverse, productive, and trophically complex marine temperate areas in the world, with Atlantic herring (*Clupea harengus*) comprising a keystone prey species, common in the diets of many marine mammals, piscivorous fish and seabirds of the region[9]. Using a large-aperture, densely sampled, coherent hydrophone array with orders of magnitude higher array gain[19] than previously available in acoustic marine mammal sensing, we could detect, localize and classify vocalizing MMs from multiple species instantaneously over an approximately 100,000 km^2 region by POAWRS[7,8] without aliasing[19] in time and space (Fig. 3a, Methods and Extended Data Figs 1–5). Simultaneous fish distributions were acquired instantaneously over tens of thousands of square kilometre areas by ocean acoustic waveguide imaging (OAWRS)[11–14], combined with conventional fisheries ultrasonic echosounding[15] and fish trawl sampling[16] to obtain thousands of calibrations at statistically significant locations[13]. We mapped the

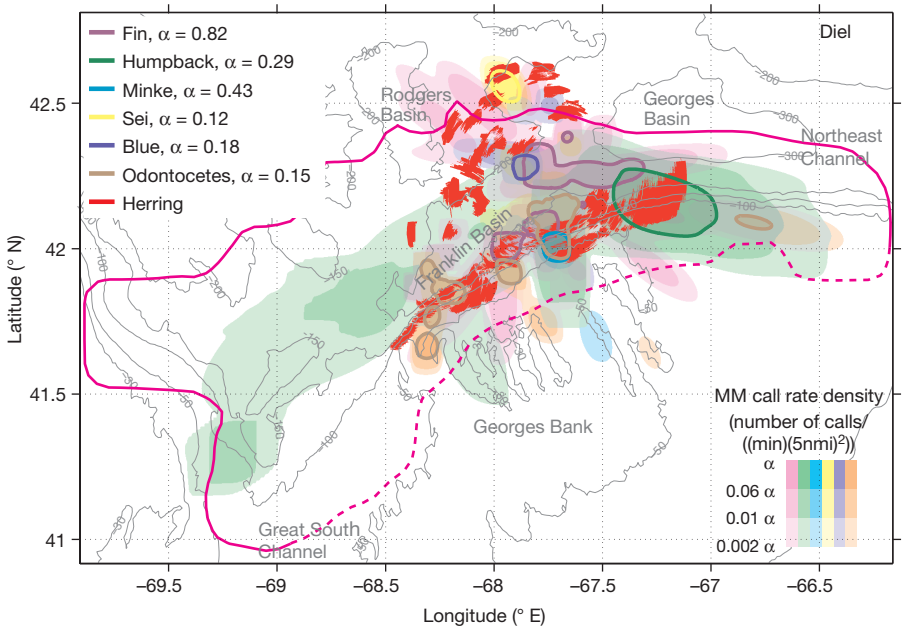

Figure 1 | Full diel cycle distributions of MM vocalizations and fish. Vocalizing MMs from diverse species are convergent on spawning herring distributions in autumn 2006 (26 September to 6 October). Dense Atlantic herring shoals (>0.2 fish per m^2, red shaded areas) imaged using OAWRS system[12,13] and diffuse herring populations (approximately 0.053 fish per m^2, bounded by magenta line) obtained from conventional fish finding sonar[15,16]. The MM call rate densities in units of number of calls per minute per 25 nmi^2 ((min)(5 nmi)^2) measured by POAWRS have peak values α indicated. Detailed shoaling herring and MM species vocalization spatial distributions can be found in Extended Data Fig. 6 and Supplementary Information section III, respectively. The bathymetric data (contours shown in grey) are obtained from the US National Centers for Environmental Information.

[1]Laboratory for Ocean Acoustics and Ecosystem Sensing, Northeastern University, 360 Huntington Avenue, Boston, Massachusetts 02115, USA. [2]Laboratory for Undersea Remote Sensing, Massachusetts Institute of Technology, 77 Massachusetts Avenue, Cambridge, Massachusetts 02139, USA. [3]Northeast Fisheries Science Center, 166 Water Street, Woods Hole, Massachusetts 02543, USA. [4]Institute of Marine Research, Post Office Box 1870, Nordnes, N-5817 Bergen, Norway.

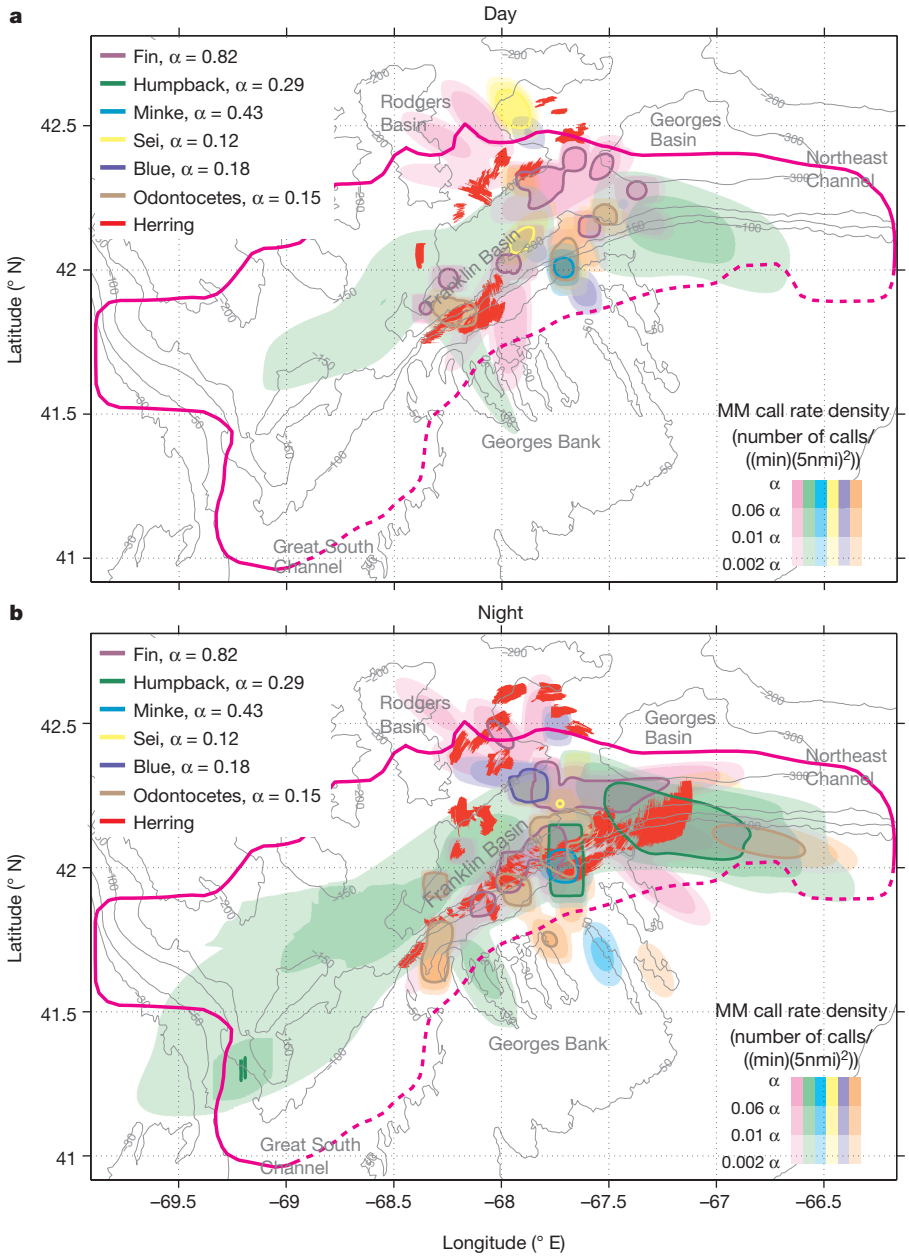

Figure 2 | Day and night distributions of MM vocalizations and fish. **a**, **b**, Daytime (**a**) and night-time (**b**) distributions of vocalizing MMs from diverse species. Regions with dense herring populations (>0.2 fish per m^2, red shaded areas) during day and night are shown. The daytime hours are between sunrise and sunset (06:00 to 18:00 EDT), while night-time hours are between sunset and sunrise the next day (18:00 to 06:00 EDT). All other contours are similar to Fig. 1. The bathymetric data (contours shown in grey) are obtained from the US National Centers for Environmental Information.

vocalization temporospatial distributions of five baleen whale species (Mysticeti): blue (*Balaenoptera musculus*), fin (*Balaenoptera physalus*), humpback (*Megaptera novaeangliae*), sei (*Balaenoptera borealis*) and minke (*Balaenoptera acutorostrata*), as well as toothed whale species (Odontoceti): sperm (*Physeter macrocephalus*), pilot (*Globicephala* spp.), orca (*Orcinus orca*) and several other delphinid species. We examined whether these vocal MMs had species-specific spatial affinities and how they varied across the prey field over the diel cycle. We further investigated the extent to which MM vocalization behaviour for each species is correlated to fish shoaling density which had recently been shown to be a major factor driving humpback vocal behaviour in their feeding ground[7].

The overall vocalization rate spatial distributions of the five baleen whale species and the toothed whales are found to be highly focused on dense herring shoaling areas[12–15] on the northern flank of Georges Bank, and almost entirely (more than 90% of the calls) contained within the region of at least diffuse herring aggregations[15,16] that extends over a roughly 12,000 km^2 area between Georges and Rodgers Basins in the north, Georges Bank in the south, Northeast Channel to the east, and Great South Channel to the west (Figs 1 and 2). The dense herring shoals[12–14] are characterized by 0.2 fish per m^2 at shoal boundaries to over 10 fish per m^2 at shoal centres, factors 4 to 200 times greater than those of the diffuse aggregations[12–15] that are characterized by roughly 0.053 fish per m^2 (Methods, Extended Data Fig. 6). The cumulative call-rate distribution for all MM species fall off rapidly with increasing range from the dense herring shoals (Fig. 3b). A significant majority of MM vocalizations from any species, at least 63% corresponding to the *e*-folding decay value of the cumulative call-rate distribution in range, originate in areas that either completely overlap with or lie within 3–8 km range

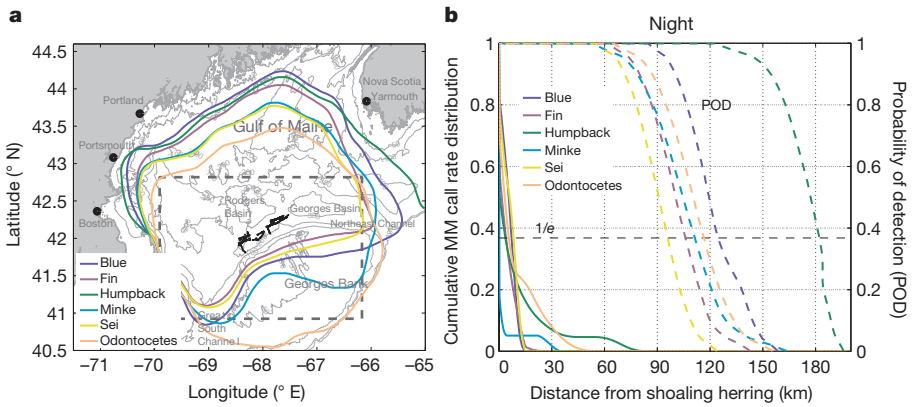

Figure 3 | POAWRS MM detection region and cumulative nocturnal MM call rate distribution. a, POAWRS 0.5 probability of detection (POD) contour for MM vocalizations in the Gulf of Maine. Dotted box is the region shown in Figs 1 and 2. **b**, Cumulative nocturnal MM vocalization rate distribution as a function of minimum distance from nocturnal herring shoaling areas. The *e*-folding distances of the cumulative nocturnal MM vocalization rate distributions range from 0–8 km depending on the species. In contrast, the azimuthally-averaged POAWRS MM POD *e*-folding distances from nocturnal herring shoaling areas are a factor of 10 to 100 times larger. The bathymetric data (contours shown in grey) are obtained from the US National Centers for Environmental Information.

of dense herring shoals. These *e*-folding distances are less than the size of the herring shoals and can be traversed by most MMs within several minutes to at most an hour, timescales small relative to the roughly 12 h duration of the herring shoal's nocturnal existence. In contrast, the zooplankton distribution in the area of intense MM vocalizations is diffuse, with volumetric densities (715 ± 550 zooplankton per m^3, Supplementary Information section V) roughly nine times smaller than those found in areas where baleen whales have been previously observed to be actively feeding[20,21] on zooplankton ($6{,}500 \pm 2{,}000$ zooplankton per m^3). From an energetics perspective, the dense herring populations, with biomass ranging from 5 g m^{-3} to over 250 g m^{-3}, provide orders of magnitude more efficient prey than the diffuse zooplankton of approximately 0.6 ± 0.5 g m^{-3} biomass. The spatial relationship quantified here between regions of dense MM vocalization rate densities and those of dense fish shoaling densities are consistent with a mechanism by which MMs from around the GOM converge on localized dense prey fields that are uniquely available during the annual herring spawning season for efficient feeding.

We find the vocal MMs are not uniformly distributed over the prey field, but concentrated in species-specific population centres with varying degrees of spatial overlap that can vary over the diel cycle depending on the species (Figs 1 and 2 and Supplementary Information section III). The dominant MM consumers of GOM herring have been proposed[9] to be fins and humpbacks, accounting for close to 50% of the estimated 150 ± 50 kilotons of herring consumed annually by MM predators, with the remaining consumed by other MM species, such as minkes and various delphinids. MMs are responsible for 50% of total herring consumption by non-human predators[9]. The Atlantic herring that spawn on northern Georges Bank comprise roughly 15% to 25% of the GOM Georges Bank complex herring stock[16]. These images reveal the previously uncharted spatial affinities of multiple MM species simultaneously engaged in foraging activities in the vicinity of an enormous fish prey field. The ability to observe predator distributions with respect to changing prey fields is essential for advancing our understanding of ecosystem processes[20,22,23].

The vocalization repertoire of MMs is highly species dependent, varying in acoustic frequency content, duration, and repetition rate (see Methods for MM species vocal classification). Of the mysticete whales, the fins are found to be the most vocal group with the highest measured vocalization rates of roughly 14,000 calls per day, followed by humpbacks with roughly 2,000 calls per day. The measured vocalization rates for all MM species are provided in Extended Data Table 1. MMs vocalize for a variety of purposes[4,5,8,23–29] that include songs associated with mating in mysticete whales, social sounds associated with inter- and intragroup interactions, signals for long range or night-time acoustic communication, calls for coordinated movement during feeding or migration, and echolocation for prey-finding in odontocetes that may possibly extend to certain mysticete whale species (Methods).

Determining the temporal and spatial variations in MM vocalizations is important for understanding their natural behaviours[4,25] and also crucial for providing controls when assessing anthropogenic effects on that behaviour[5]. All five baleen whale species and the toothed whales analysed here have vocalization rates that vary over the diel cycle. Four of the five baleen whale species, fin, humpback, blue and minke, are found to be more vocal at night (from dusk 18:00 Eastern daylight time (EDT) through to dawn 06:00 EDT the next day) with night-time vocalization rates a factor of between 2 to 10 times that of the daytime (Extended Data Table 1). In contrast, the sei whales and collectively, the odontocetes, are more vocal in the daytime by a factor of roughly 1.25. The vocalization rate spatial distribution is strongly diel-dependent for some MM species, but less so for others (Fig. 2a, b). Combined sensing with POAWRS and OAWRS[7,8,11–14] enables MM and fish distributions to be simultaneously monitored over instantaneous continental-shelf scale regions, and presents a significant advantage in areal coverage over conventional line-transect visual[10,30] and ultrasonic echosounding survey techniques respectively.

We correlated the MM vocalization rate time series with the herring shoaling areal population density time series over the diel cycle as a function of MM species (Fig. 4, Extended Data Fig. 7 and Extended Data Table 1). Four of the five vocal baleen whale species, fin, humpback, minke and blue, are found to have temporal call rate trends that are highly correlated to temporal trends in herring shoaling density and also to each other. For humpbacks, their night-time vocalizations are dominated by downsweep 'meows', 'feeding cries'and 'bow-shaped' calls that are associated with fish-feeding activities, occur ten times more frequently at night than in the daytime accounting for the high correlation ($r_{MM,fish} = 0.87$) to nocturnal herring shoaling densities[7]. The high temporal correlation ($r_{MM,fish} = 0.82$) obtained here between fin vocalization rate and herring shoaling density indicates that the factor of 2 increase in the characteristic 20 Hz fin vocalizations at night is likely associated with increased fish-feeding activities. This is supported by the spatial focusing of the fin vocalization distribution on north-central Georges Bank in the location of dense herring shoaling populations during night-time (Fig. 2). The minke vocalization rates are well correlated to herring shoaling densities, both temporally ($r_{MM,fish} = 0.64$) and spatially. The minke call rate distribution spatial overlap with dense herring shoaling areas increases from 0% in the day to 71% at night (Fig. 3b and Extended Data Fig. 8). This implies

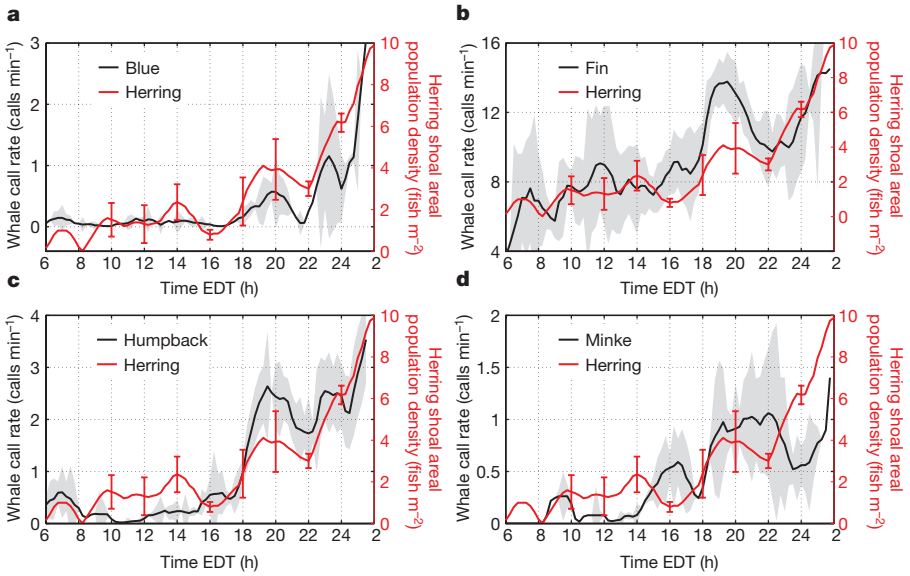

Figure 4 | Diel MM call rate and herring shoal areal population density time series. a–d, Mean call rates for blue (**a**), fin (**b**), humpback (**c**), and minke (**d**) whales are correlated to Atlantic herring shoal mean areal population density over the diel cycle. The error bars indicate standard deviations obtained from averaging the time series over multiple diel cycles from 26 September to 6 October 2006. The period from roughly 2–6 EDT contains a data gap.

that the fivefold increase in minke buzz vocalization sequences recorded here, which resemble the odontocete echolocation click sequences (compare Extended Data Fig. 1d, e), play an important role in minke fish-feeding activity. Here we find the blue vocalization rates have the highest temporal correlation ($r_{MM,fish} = 0.91$) to herring shoaling densities. The blue whale calls we detected are comprised predominantly of short-duration (approximately 2 s) audible downsweep (type D[26]) calls, which were previously observed for blue whales in both the North Atlantic[26] and Pacific feeding grounds[27] and regarded as contact calls. The high temporal correlation between blue whale call rates and herring densities obtained here suggest that it may be possible that blue whales are consuming herring and the type D vocalizations are feeding-related, though this fish-feeding behaviour has not been observed for blue whales. (Other possible explanations are discussed in Methods.) Previous observations of sei whales in the GOM found lower call rates at night for their downsweep chirp signals attributed to zooplankton-feeding and higher call rates in the daytime while engaged in social interactions and less feeding[23]. Here we find a similar pattern for their vocalization behaviour in the vicinity of dense herring shoals, which may result from more fish-feeding at night than in daytime. The tooth whales collectively have vocalization rates that are temporally uncorrelated to herring shoaling densities, perhaps because their fish-feeding strategies differ from those of baleen whales. The toothed whales hunt small fish groups and feed on individual fish[28,29], whereas baleen whales engulf large quantities, hundreds to thousands of fish, all at once[24] and rely on fish shoaling together for efficient feeding.

The ecosystem-scale predator–prey behaviour documented here is expected to be a regular feature of the annual herring spawning season on Georges Bank and an important aspect of the life cycles of the various species involved that is likely to be found in other ocean ecosystems where many of the same conditions occur.

Online Content Methods, along with any additional Extended Data display items and Source Data, are available in the online version of the paper; references unique to these sections appear only in the online paper.

Received 19 June; accepted 21 December 2015.
Published online 2 March 2016.

1. Tittensor, D. P. *et al.* Global patterns and predictors of marine biodiversity across taxa. *Nature* **466,** 1098–1101 (2010).
2. Schofield, O. *et al.* How do polar marine ecosystems respond to rapid climate change? *Science* **328,** 1520–1523 (2010).
3. Block, B. A. *et al.* Tracking apex marine predator movements in a dynamic ocean. *Nature* **475,** 86–90 (2011).
4. Noad, M., Cato, D., Bryden, M., Jenner, M. & Jenner, K. Cultural revolution in whale songs. *Nature* **408,** 537 (2000).
5. Miller, P. J., Biassoni, N., Samuels, A. & Tyack, P. L. Whale songs lengthen in response to sonar. *Nature* **405,** 903 (2000).
6. Kaschner, K., Quick, N. J., Jewell, R., Williams, R. & Harris, C. M. Global coverage of cetacean line-transect surveys: status quo, data gaps and future challenges. *PLoS ONE* **7,** e44075 (2012).
7. Gong, Z. *et al.* Ecosystem scale acoustic sensing reveals humpback whale behavior synchronous with herring spawning processes and re-evaluation finds no effect of sonar on humpback song occurrence in the Gulf of Maine in fall 2006. *PLoS ONE* **9,** e104733 (2014).
8. Tran, D. D. *et al.* Using a coherent hydrophone array for observing sperm whale range, classification, and shallow-water dive profiles. *J. Acoust. Soc. Am.* **135,** 3352–3363 (2014).
9. Overholtz, W. J. & Link, J. S. Consumption impacts by marine mammals, fish, and seabirds on the Gulf of Maine–Georges Bank Atlantic herring (*Clupea harengus*) complex during the years 1977–2002. *ICES J. Mar. Sci.* **64,** 83–96 (2007).
10. Waring, G. T., Josephson, E., Maze-Foley, K. & Rosel, P. E. U.S. Atlantic and Gulf of Mexico Marine Mammal Stock Assessments 2014. *NOAA Tech Memo NMFS NE* Vol. 231 (2014).
11. Makris, N. C. *et al.* Fish population and behavior revealed by instantaneous continental shelf-scale imaging. *Science* **311,** 660–663 (2006).
12. Makris, N. C. *et al.* Critical population density triggers rapid formation of vast oceanic fish shoals. *Science* **323,** 1734–1737 (2009).
13. Gong, Z. *et al.* Low-frequency target strength and abundance of shoaling Atlantic herring (*Clupea harengus*) in the Gulf of Maine during the ocean acoustic waveguide remote sensing 2006 experiment. *J. Acoust. Soc. Am.* **127,** 104–123 (2010).
14. Jagannathan, S. *et al.* Ocean acoustic waveguide remote sensing (OAWRS) of marine ecosystems. *Mar. Ecol. Prog. Ser.* **395,** 137–160 (2009).
15. Jech, J. M. & Stroman, F. Aggregative patterns of pre-spawning Atlantic herring on Georges Bank from 1999–2010. *Aquat. Living Resour.* **25,** 1–14 (2012).
16. 54th Northeast Regional Stock Assessment Workshop (54th SAW) Assessment Report. Part A. Atlantic herring stock assessment for 2012. *US Dept Commer, Northeast Fish Sci. Cent.* Ref. Doc. 12–18; 600 p. http://www.nefsc.noaa.gov/publications/ (2012).
17. deYoung B., Heath, M., Werner, F., Chai, F., Megrey, B. & Monfray, P. Challenges of modeling ocean basin ecosystems. *Science* **304,** 1463–1466 (2004).
18. Overholtz, W. & Link, J. A simulation model to explore the response of the Gulf of Maine food web to large-scale environmental and ecological changes. *Ecol. Modell.* **220,** 2491–2502 (2009).
19. Kay, S. M. Fundamentals of statistical signal processing, Vol. II: Detection Theory. (Prentice Hall, 1998).
20. Mayo, C. A. & Marx, M. K. Surface foraging behavior of the North Atlantic right whale, *Eubalaena glacialis*, and associated zooplankton characteristics. *Can. J. Zool.* **68,** 2214–2220 (1990).

21. Dolphin, W. F. Prey densities and foraging of humpback whales, *Megaptera novaeangliae. Experientia* **43,** 468–471 (1987).
22. Sims, D. W. & Quayle, V. A. Selective foraging behavior of basking sharks on zooplankton in a small scale front. *Nature* **393,** 460–464 (1998).
23. Baumgartner, M. F. & Frantantoni, D. M. Diel periodicity in both sei whale vocalization rates and the vertical migration of their copepod prey observed from ocean gliders. *Limnol. Oceanogr.* **53,** 2197–2209 (2008).
24. Nøttestad, L., Fern, A., Mackinson, S., Pitcher, T. & Misund, O. A. How whales influence herring school dynamics in a cold-front area of the Norwegian Sea. *ICES J. Mar. Sci.* **59,** 393–400 (2002).
25. Janik, V. M. Whistle matching in wild bottlenose dolphins (*Tursiops truncatus*). *Science* **289,** 1355–1357 (2000).
26. Berchok, C. L., Bradley, D. L. & Gabrielson, T. B. St. Lawrence blue whale vocalizations revisited: characterization of calls detected from 1998 to 2001. *J. Acoust. Soc. Am.* **120,** 2340–2354 (2006).
27. Wiggins, S. M., Oleson, E. M., McDonald, M. A. & Hildebrand, J. A. Blue whale (*Blaenoptera musculus*) diel call patterns offshore of Southern California. *Aquat. Mamm.* **31,** 161–168 (2005).
28. Similä, T. Sonar observations of killer whales *(Orcinus orca)* feeding on herring schools. *Aquat. Mamm.* **23,** 119–126 (1997).
29. Wiirsig, B. Delphinid foraging strategies in *Dolphin cognition and Behavior: a Comparative Approach* 347–359 (Psychology Press, 1986).
30. Buckland, S. T. *et al. Introduction to Distance Sampling: Estimating Abundance of Biological Population* (Oxford Univ. Press, 2001).

Supplementary Information is available in the online version of the paper.

Acknowledgements Permission for this National Oceanographic Partnership Program experiment was given in the Office of Naval Research document 5090 Ser 321RF/096/06. This research was supported by the US National Science Foundation, the US Office of Naval Research (Ocean Acoustics Program), the National Oceanographic Partnership Program, the US Presidential Early Career Award for Scientists and Engineers, the Alfred P. Sloan Foundation, the Census of Marine Life, and Northeastern University. The authors thank J. R. Preston for assistance with GOM 2006 experiment, D. H. Cato and P. L. Tyack for discussions.

Author Contributions Overall concept and approach conceived and developed by P.R. Implementation, data analysis and interpretation directed by P.R., conducted by D.W., W.H., H.G. and D.D.T. with contributions from A.D.J., D.H.Y. and Z.G. The GOM 2006 experiment data collection was led by N.C.M., P.R. and J.M.J. The article was written by P.R. with contributions from D.W., W.H., J.M.J., O.R.G. and N.C.M. All authors read and discussed the manuscript.

Author Information Reprints and permissions information is available at www.nature.com/reprints. The authors declare no competing financial interests. Readers are welcome to comment on the online version of the paper. Correspondence and requests for materials should be addressed to P.R. (purnima@ece.neu.edu).

METHODS

Data reporting. No statistical methods were used to predetermine sample size. The investigators were not blinded to allocation during experiments and outcome assessment.

POAWRS receiver array recordings of MM vocalizations. Acoustic recordings were acquired using a 160 hydrophone-element horizontal receiver line-array[31] towed by a research vessel along designated tracks north of Georges Bank from 19 September to 6 October 2006 (GOM 2006 experiment)[11–14], coinciding with the annual herring spawning period[15,16,32] on the northern flank of Georges Bank[9,33,34]. Here we use data from all 160 hydrophone elements nested[13,31] into four subapertures, where each subaperture contains 64 hydrophones for spatially and temporally unaliased sensing up to 4 kHz (sampling rate of POAWRS was 8 kHz)[35]. Acoustic pressure-time series measured by sensors across the receiver array were converted to two-dimensional (2D) beam-time series by time-domain beamforming[19,36], and further converted to spectrograms by temporal Fourier transform. MM vocalizations were automatically extracted using a threshold detector (>5.6 dB signal-to-noise ratio (SNR)) with a detection rate of roughly 87% ± 5% depending on the species, call characteristics and in-beam ambient noise levels. The beamformed spectrograms were subsequently checked by visual inspection to improve expected detection accuracy to over 92%. Examples of typical vocalization spectrogram from diverse MM species are shown in Extended Data Fig. 1.

The high gain[19,36] of the densely-sampled large aperture coherent POAWRS receiver array used here, up to 10 $\log_{10}$ $n = 18$ dB gain where $n = 64$ hydrophones for each sub-aperture, enabled detection of whale vocalizations either two orders of magnitude more distant in range or lower in SNR than a single hydrophone which has no array gain (Extended Data Fig. 2). The angular resolution of the receiver array[12] is dependent on the measured bearing, array aperture length and acoustic wavelength, tabulated in Table 1 of ref. 13 for select frequencies.

Characteristics and function of MM vocalizations from diverse species. The time-frequency characteristics of each MM vocalization was extracted via pitch tracking[37–39] and applied to classify the vocalization according to species (Extended Data Fig. 3 and Extended Data Table 2). A combination of extracted features, orthogonalized via principle component analysis (PCA), were used to optimize the vocalization species classification employing *k*-means and Bayesian-based Gaussian mixture model clustering approaches[40]. The bearing-time trajectories of each closely associated series of vocalizations were also taken into account to ensure consistent classification, and to minimize the automatic classification error to between 0.5% to 7% depending on the species.

In the low frequency range from 10 Hz to 100 Hz, the acoustic spectra were dominated by fin, blue and sei vocalizations (Extended Data Fig. 1a–c). The fins were identified from their characteristic 20 Hz centre frequency calls[41–44] that have been associated with communication among fin individuals[45] and also found to be uttered by males as breeding displays in their mating grounds[41,46]. Given the large volume of fin vocalizations measured here in the vicinity of dense shoaling fish populations, averaging 14,000 calls per day, these 20 Hz calls can also be associated with feeding behaviour, serving as communication signals or for coordination among individuals in their foraging ground. The blues were identified from their audible downsweeps — type D calls, burps and grunts[26,47–50], previously found to be vocalized by both sexes, regarded as contact or social calls[48] produced by individuals at shallow depths[47] of 10–40 m. The seis were identified from their downsweep calls occurring singly or as doublets with roughly 4 s separation, and also sometimes as triplets[23,51,52], hypothesized to be long-range contact calls potentially enabling coordinated activities such as feeding or breeding[52].

The spectra in the mid frequency range from 100 Hz to 1,000 Hz were dominated by minke and humpback vocalizations. The minkes were identified from their buzzes comprised of a series of high and low frequency click sequences[53–55], has characteristics similar to the highly repetitive pulse train of odontocetes that may be suitable for prey echolocation. Compared to other baleen whales, the humpbacks have a fairly extensive vocalization repertoire. Here the humpbacks were identified from their songs[4,56], as well as non-song calls[57,58] with characteristics provided in ref. 7. Male humpbacks vocalize songs which are patterned sequences of calls as breeding displays[4] in their mating ground, and have been observed to carry the tunes into their feeding grounds[59–61] (Extended Data Fig. 2). The non-song vocalizations detected include 'feeding cries' similar to those observed in Alaskan humpback cooperative group feeding on herring schools[57], as well as 'bow-shaped' calls and 'meows' suited for night time communication[7] among humpback individuals and coordination during group feeding activities.

The spectra at frequencies higher than 1 kHz were dominated by odontocete vocalizations (Extended Data Fig. 1e–h). They consist of sperm whale slow and usual click, and creak sequences[8,62,63], pilot and killer whale whistles, as well as a wide range of repetitive sequences of downsweep chirp signals roughly 0.7 s duration with varying bandwidths between 200 to 1,000 Hz, all occurring above 1 kHz that can be attributed to pilot[64,65] or killer whales[66–68], or a variety of other delphinid species[25]. The highly repetitive click sequences used for prey echolocation occur at frequencies higher than 10 kHz for many odontocete species, beyond our sampling frequency range. The largest of them, the sperm whale, has slow and usual click and creak sequences with significant energy as low as 1 kHz[8,69]. The whistles and wide variety of downsweep chirp signals we recorded in the frequency range of odontocete vocalizations may serve as contact calls between individuals and to facilitate cohesion during foraging or travel[64,65,70]. The fin, humpback, sei, minke, pilot and orca whales, and common and bottlenose dolphin species were visually sighted during the experiment.

Determination of diel MM vocalization rate time series. The bearing-time trajectories of vocalizations from multiple MM species received by the POAWRS receiver array are shown for two days in Extended Data Fig. 4. For humpbacks, the alternation from song to non-song calls in their vocalization repertoire over several diel cycles are plotted as a function of bearing-time trajectory in Extended Data Fig. 5 for comparison. The line-array's left–right ambiguity is resolved following the approach outlined in refs. 7, 71. The bearing ranges from 100° to 240° from true north for our array spans Georges Bank from east to west respectively. The diel vocalization rate (calls per min) time series shown in Fig. 4 and Extended Data Fig. 7 for each MM species is obtained by averaging the daily vocalization rate time series for that species over the entire experiment. The MM vocalization rate time series, initially calculated in 15 min bins, are averaged over a 1.25 h running window corresponding to the half power width quantifying the temporal correlation scale of the fish shoaling density time series. For both minke and odontocete whale click sequences, since the duration of each click sequence is highly variable from a few seconds to over a minute, the call rates shown in Fig. 4 and Extended Data Fig. 7 represent the number of 5 s intervals that contain click sequences.

Localization and call rate spatial distributions of diverse vocalizing MM species. The horizontal location of each MM vocalization consists of a range and a bearing estimate. The moving array triangulation (MAT)[71] and the array invariant (AI)[71–73] methods were applied to determine the range of the vocalizations from the horizontal receiver array centre. Position estimation error, or the root mean squared (RMS) distance between the actual and estimated location, is a combination of range and bearing errors quantified for this array in refs. 7, 71 and 73. Range estimation error, expressed as the percentage of the range from the source location to the horizontal receiver array centre, for the MAT technique is roughly 2% at array broadside and gradually increases to 10% at 65° from broadside and 25% at 90° from broadside, that is, near or at endfire[71]. Range estimation error for the AI method is roughly 4% to 8% over all azimuthal directions[71,73]. Bearing estimation error of the time domain beamformer is roughly 0.5° at broadside and gradually increases to 6.0° at endfire[71]. These errors are determined at the same experimental site and time period as the MM position estimates presented here, from thousands of controlled source signals transmitted by the same source array used to locate the herring shoals presented here and are based on absolute global positioning system (GPS) ground truth measurements of the source array's position[71], which are accurate to within 3 m to 10 m. More than 80% of vocalizing MMs are found to be located between 0° to 65° from the broadside direction of the horizontal receiver array. Position estimation error[7,71] is less than 2 km for majority of the vocalizing MMs localized in Figs 1 and 2 since they are found within roughly 50 km of the horizontal receiver array centre. This error is over an order of magnitude smaller than the spatial scales of the MM concentrations shown in Figs 1 and 2, and consequently has negligible influence on the analyses and results.

The estimated locations for all MM calls over the duration of our data collection are used to generate the call rate density map for each MM species shown in Figs 1 and 2 following the approach described in ref. 7. The location of each call is characterized by a 2D Gaussian probability density function with mean equal to the measured mean position from MAT or the AI method and standard deviations determined by the measured range and bearing standard deviations. The MM call rate density map for each species is determined by superposition of the 2D spatial probability densities for the location of each call, normalized by the total measurement time. (See Supplementary Information section III for more detailed diel, diurnal and nocturnal MM spatial vocalization rate distributions).

Estimating MM detection region for POAWRS receiver array. The probability of detection $P_D(r)$ of the MM vocalizations from each species as a function of range r from the POAWRS receiver array, shown in Fig. 3 and Extended Data Fig. 8, are calculated employing the formulation[7,13,74–86] and parameters[7,87–89] provided in Supplementary Information section I. Higher transmission loss occurs in shallower waters due to more intense and pervasive bottom interaction[86,90–92] and mode stripping effects, especially at the low frequency vocalization range of large baleen whales. Transmission loss in deeper waters is typically significantly lower due to upward refraction[86,90] which leads to far less intense and pervasive bottom

interaction, as is the case in the deeper waters north of Georges Bank[86,90–92]. As noted in ref. 7, highly directional transmission loss may then occur when there are large depth variations about a receiver. This effect makes the detection range of whales in directions to the north of our receiver and Georges Bank typically much greater than in directions to its south where the relatively shallow waters of Georges Bank are found. The fact that we localized the sources of many whale calls at great distances along shallow water propagation paths on Georges Bank in directions where transmission loss was greater and found negligibly small vocalization rates in the deeper waters north of Georges Bank where transmission loss was much less (Fig. 3a), greatly emphasizes the finding that the vocalization rates originating from the region further north of Georges Bank were negligibly small.

The dominant portion of the whale population within the POAWRS detection region is expected to occur in areas with dense vocalization rates for each MM species. This is because the probability of detecting no vocalizations in a region where a MM species is abundant over our two week observation period is negligibly small. This implies that there are insignificant numbers of MMs within the detection region at locations with low call rates or no calls. This is consistent with acoustic-based marine mammal population density estimation, which makes the standard assumption that there are no whales expected to be present in a time-space region where there are no calls[93–98], or that this number is negligibly small. The MM vocalization rate spatial distribution obtained here showing the northern flank of Georges Bank and its immediate vicinity as an autumn season MM hotspot is consistent with analysis of three decades (1970–2005) of visual line transect survey data for the entire GOM region[10,99] (Supplementary Information section IV).

Atlantic herring areal population density distribution and time series. The Atlantic herring instantaneous areal population density over wide areas shown in Figs 1 and 2 and Extended Data Fig. 6 were obtained from active OAWRS imaging after extensive calibration with tens of thousand instantaneous coincident conventional ultrasonic fisheries echosounding measurements[12–14], with fish species identification and physiological parameters extracted from trawl samples collected over the course of the experiment[15]. The Atlantic herring shoals were consistently observed to form when the population density reached a critical value of 0.2 fish per m^2 where correlated behaviour began, following simple physical theories[12]. This critical density was also consistently found to be the boundary where the dense shoal ended and diffuse populations that did not engage in correlated behaviour began[12–14]. Populations within the dense shoals were variable from 0.2 to over 10 fish per m^2. These shoals extended roughly 20–60 m vertically in water-column depths of 80–200 m. In contrast, the diffuse fish populations approximately 0.053 fish per m^2 were found close to (within 3–5 m of) the seafloor. The shoals formed near sunset and persisted until near sunrise, starting on the northern flank of Georges Bank and migrating southward to shallower waters on the bank. This diurnal behavioural pattern was consistently observed during our roughly two week measurement time period[12–14].

The annual autumn season Atlantic herring spawning activity on the northern flank of Georges Bank has been recorded by the US National Marine Fisheries Services (NMFS) for over 30 years, coinciding their survey of the Georges Bank herring stock with this period each year[9,15,16,32], including our GOM 2006 experiment. The overall Georges Bank Atlantic herring stock estimate for autumn 2006 based on OAWRS[16] survey has been found to match well (within 10% to 20%) with independent NMFS stock estimates for 2006 and 2007 (ref. 16).

Midwater trawl hauls were conducted on an ad hoc basis to sample significant backscatter observed during the NMFS acoustic survey in autumn 2006 (ref. 15). Stomach-content volume and diet composition of up to 15 herring per trawl haul (length-stratified subsampling) were recorded at sea. The majority of pre-spawning herring were not feeding as evidenced by the high proportion of empty stomachs[15]. During the acoustic/midwater trawl survey on Georges Bank in 2006, 95% of herring had nothing in their stomach (that is, stomach-content volume was 0 cm^3), which is comparable to other years where the proportion of empty stomachs ranged from 100% in 2003 to 69% in 2010.

The areal resolution of the fish density distribution shown in Figs 1 and 2 obtained from the OAWRS imaging system is 30 m in range after matched filtering and averaging, and varies between 150 m to roughly 1.5 km in cross-range for the vast majority of fish hotspots included here, where the cross-range resolution is dependent on the array angular resolution, bearing, and fish range. The MM call rate distributions have spatial resolutions bounded by roughly 2 km that is of the same order of magnitude as the fish areal population density distribution in cross range.

We combine the herring shoaling activity on Georges Bank, where massive and highly dense shoals occur predominantly during the night on the northern flank[7,8,11–14], with that for the region to the north of the Bank between Rodgers and Georges Basins, where we observe less persistent herring groups forming throughout the diel cycle[15]. The areal fish population density (in fish/m^2) time series shown Fig. 4 and Extended Data Fig. 7 is obtained by averaging the daily herring shoaling areal population density time series initially calculated in 15 min bins, then averaged over a 1.25 h running window corresponding to the half power width quantifying the temporal correlation scale of the fish shoaling density time series.

The temporal correlation coefficients $r_{\mathrm{MM,fish}}$ in Extended Data Table 1 quantify the degree of similarity between the diel MM call rate time series $c_{\mathrm{MM}}(t)$ and the diel fish areal population density time series $n_{\mathrm{fish}}(t)$ and are calculated[19,100] via

$$r_{MM,fish} = \frac{\sum_{k=1}^{N}(c_{MM}(t_k) - \overline{c_{MM}})(n_{fish}(t_k) - \overline{n_{fish}})}{\sqrt{\sum_{k=1}^{N}(c_{MM}(t_k) - \overline{c_{MM}})^2}\sqrt{\sum_{k=1}^{N}(n_{fish}(t_k) - \overline{n_{fish}})^2}} \quad (1)$$

using measurements $c_{\mathrm{MM}}(t_j)$ and $c_{\mathrm{MM}}(t_k)$ that are independent for $j \neq k$, so that $t_{k+1} - t_k = 1.25$ h. Similarly, the temporal correlation coefficient $r_{\mathrm{MMI,MMII}}$ between the diel call rate time series of two distinct MM species is calculated via,

$$r_{MM_I,MM_{II}} = \frac{\sum_{k=1}^{N}(c_{MM_I}(t_k) - \overline{c_{MM_I}})(c_{MM_{II}}(t_k) - \overline{c_{MM_{II}}})}{\sqrt{\sum_{k=1}^{N}(c_{MM_I}(t_k) - \overline{c_{MM_I}})^2}\sqrt{\sum_{k=1}^{N}(c_{MM_{II}}(t_k) - \overline{c_{MM_{II}}})^2}} \quad (2)$$

where the samples at time t_j and t_k are independent for $j \neq k$, so that $t_{k+1} - t_k = 1.25$ h.

The cumulative MM call rate distributions in Fig. 3b and Extended Data Fig. 8 are plotted as functions of decreasing distance from shoaling herring during night and day respectively, and so take the value 0 at long ranges from herring shoaling locations and monotonically increase to 1 at herring shoaling locations. The probability density function (PDF) for MM call rate density as a function of range from shoaling herring can be obtained as the absolute value of the range—derivative of the cumulative call rate distribution. The e-folding decay range of the cumulative call rate distribution for each MM species is the distance from herring shoals where the cumulative call rate distribution decays to $1/e = 0.37$, so that 63% of vocalizations from that species are contained within the e-folding decay range.

On the high temporal correlation between blue whale vocalization rate and herring shoaling density. Besides the fish-feeding hypothesis, another possible explanation is that both blue whales and herring are responding to a common environmental stimulus, such as changing light level or their common prey-zooplankton abundance. However, the annual biological sampling of the autumn season spawning herring over multiple years, including this 2006 experiment time period, indicates that the herring have largely empty stomachs and are generally not feeding while engaged in spawning activities[15].

Previous studies of diel dependence of blue vocalizations in their zooplankton-feeding areas found higher call rates in the night than day for longer duration (approximately 20 s) type B calls, associated with mating and social interaction, and proposed an inverse relationship between call rate and level of feeding activity[27]. It is also possible that the type D calls measured here are related to increased social interaction between blue whales at night.

The Supplementary Information provides more details on marine mammal, fish and zooplankton distributions in GOM and comparison to other ocean environments.

31. Becker, K. & Preston, J. R. The ONR five octave research array (FORA) at Penn State. *Proc. OCEANS '03* **5**, 26072610 (2003).
32. Overholtz, W. J. *et al.* Stock assessment of the Gulf of Maine-Georges Bank Atlantic herring complex, 2003. *Northeast Fisheries Science Center References Document* **4,** 1–290 (2004).
33. Melvin, G. D. & Stephenson, R. L. The dynamics of a recovering fish stock: Georges Bank herring. *ICES J. Mar. Sci.* **64,** 69–82 (2007).
34. Read, A. J. & Brownstein, C. R. Considering other consumers: fisheries, predators, and Atlantic herring in the Gulf of Maine. *Conserv. Ecol.* **7,** 2 (2003).
35. Oppenheim, A. V., Willsky, A. S. & Nawab, S. H. *Signals and Systems* (PrenticeHall, 1997).
36. Johnson, D. H. & Dudgeon, D. E. *Array Signal Processing: Concepts and Techniques* (Simon & Schuster, 1992).
37. Baumgartner, M. F. *et al.* A generalized baleen whale call detection and classification system. *J. Acoust. Soc. Am.* **129,** 2889–2902 (2011).
38. Shapiro, A. D. & Wang, C. A versatile pitch tracking algorithm: From human speech to killer whale vocalizations. *J. Acoust. Soc. Am.* **126,** 451–459 (2009).
39. Wang, C. & Seneff, S. Robust pitch tracking for prosodic modeling in telephone speech. *Proceedings of the IEEE International Conference on Acoustics, Speech, and Signal Processing* (IEEE, Piscataway, NJ) 1143–1145 (2000).
40. Duda, R. O., Hart, P. E. & Stork, D. G. *Pattern Classification* 2nd edn (John Wiley & Sons, 2001).

41. Watkins, W. A., Tyack, P., Moore, K. E. & Bird, J. E. The 20-Hz signals of finback whales (*Balaenoptera physalus*). *J. Acoust. Soc. Am.* **82,** 1901–1912 (1987).
42. Edds, P. L. Characteristics of finback *Balaenoptera physalus* vocalizations in the St. Lawrence Estuary. *Bioacoustics* **1,** 131–149 (1988).
43. Nieukirk, S. L. *et al.* Sounds from airguns and fin whales recorded in the mid-Atlantic Ocean, 1999–2009. *J. Acoust. Soc. Am.* **131,** 1102–1112 (2012).
44. Thompson, P. O., Findley, L. T. & Vidal, O. 20 Hz pulses and other vocalizations of fin whales, *Balaenoptera physalus*, in the Gulf of California, Mexico. *J. Acoust. Soc. Am.* **92,** 3051–3057 (1992).
45. McDonald, M. A., Hildebrand, J. A. & Webb, S. C. Blue and fin whales observed on a seafloor array in the Northeast Pacific. *J. Acoust. Soc. Am.* **98,** 712–721 (1995).
46. Croll, D. A. *et al.* Only male fin whales sing loud songs. *Nature* **417,** 809 (2002).
47. Oleson, E. M. Behavioral context of call production by eastern North Pacific blue whales. *Mar. Ecol. Prog. Ser.* **330,** 269–284 (2007).
48. McDonald, M. A., Calambokidis, J., Teranishi, A. M. & Hildebrand, J. A. The acoustic calls of blue whales off California with gender data. *J. Acoust. Soc. Am.* **109,** 1728–1735 (2001).
49. Thode, A. M., D'Spain, G. L. & Kuperman, W. A. Matched-field processing, geoacoustic inversion, and source signature recovery of blue whale vocalizations. *J. Acoust. Soc. Am.* **107,** 1286–1300 (2000).
50. Di Iorio, L. & Clark, C. W. Exposure to seismic survey alters blue whale acoustic communication. *Biol. Lett.* **6,** 51–54 (2010).
51. Rankin, S. & Barlow, J. Vocalizations of the sei whale *Balaenoptera borealis* off the Hawaiian Islands. *Bioacoustics* **16,** 137–145 (2007).
52. Baumgartner, M. F. *et al.* Low frequency vocalizations attributed to sei whales (*Balaenoptera borealis*). *J. Acoust. Soc. Am.* **124,** 1339–1349 (2008).
53. Edds-Walton, P. L. Vocalizations of minke whales *Balaenoptera acutorostrata* in the St. Lawrence Estuary. *Bioacoustics* **11,** 31–50 (2000).
54. Mellinger, D. K., Carson, C. D. & Clark, C. W. Characteristics of minke whale (*Balaenoptera acutorostrata*) pulse trains recorded near Puerto Rico. *Mar. Mamm. Sci.* **16,** 739–756 (2000).
55. Risch, D. *et al.* Minke whale acoustic behavior and multi-year seasonal and diel vocalization patterns in Massachusetts Bay, USA. *Mar. Ecol. Prog. Ser.* **489,** 279–295 (2013).
56. Payne, R. S. & McVay, S. Songs of humpback whales. *Science* **173,** 585–597 (1971).
57. Cerchio, S. & Dahlheim, M. Variation in feeding vocalizations of humpback whales (*Megaptera novaeangliae*) from southeast Alaska. *Bioacoustics* **11,** 277–295 (2001).
58. Cato, D., McCauley, R., Rogers, T. & Noad, M. Passive acoustics for monitoring marine animals-progress and challenges. *Proceedings of Acoustics* **2006,** 453–460 (2006).
59. Mattila, D. K., Guinee, L. N. & Mayo, C. A. Humpback whale songs on a North Atlantic feeding ground. *J. Mamm.* **68,** 880–883 (1987).
60. McSweeney, D. J., Chu, K. C., Dolphin, W. F. & Guinee, L. N. North Pacific humpback whale songs: a comparison of southeast Alaskan feeding ground songs with Hawaiian wintering ground songs. *Mar. Mamm. Sci.* **5,** 139–148 (1989).
61. Clark, C. W. & Clapham, P. J. Acoustic monitoring on a humpback whale (*Megaptera novaeangliae*) feeding ground shows continual singing into late spring. *Proc. Royal Soc. B* **271,** 1051–1057 (2004).
62. Watkins, W. A. & Schevill, W. E. Sperm whale codas. *J. Acoust. Soc. Am.* **62,** 1485–1490 (1977).
63. Tiemann, C. O., Thode, A. M., Straley, J., O'Connell, V. & Folkert, K. Three-dimensional localization of sperm whales using a single hydrophonea. *J. Acoust. Soc. Am.* **120,** 2355–2365 (2006).
64. Nemiroff, L. & Whitehead, H. Structural characteristics of pulsed calls of long-finned pilot whales *Globicephala melas*. *Bioacoustics* **19,** 67–92 (2009).
65. Weilgart, L. S. & Whitehead, H. Vocalizations of the North Atlantic pilot whale (*Globicephala melas*) as related to behavioral contexts. *Behav. Ecol. Sociobiol.* **26,** 399–402 (1990).
66. Tyson, R. B., Nowacek, D. P. & Miller, P. J. Nonlinear phenomena in the vocalizations of North Atlantic right whales (*Eubalaena glacialis*) and killer whales (*Orcinus orca*). *J. Acoust. Soc. Am.* **122,** 1365–1373 (2007).
67. Simon, M., Ugarte, F., Wahlberg, M. & Miller, L. A. Icelandic killer whales *Orcinus orca* use a pulsed call suitable for manipulating the schooling behaviour of herring *Clupea harengus*. *Bioacoustics* **16,** 57–74 (2006).
68. Filatova, O. A. *et al.* Call diversity in the North Pacific killer whale populations: implications for dialect evolution and population history. *Anim. Behav.* **83,** 595–603 (2012).
69. Oliveira, C., Wahlberg, M., Johnson, M., Miller, P. J. & Madsen, P. T. The function of male sperm whale slow clicks in a high latitude habitat: communication, echolocation, or prey debilitation? *J. Acoust. Soc. Am.* **133,** 3135–3144 (2013).
70. Ford, J. K. Acoustic behavior of resident killer whales (*Orcinus orca*) off Vancouver Island, British Columbia. *Can. J. Zool.* **67,** 727–745 (1989).
71. Gong, Z., Tran, D. & Ratilal, P. Comparing passive source localization and tracking approaches with a towed horizontal receiver array in an ocean waveguide. *J. Acoust. Soc. Am.* **134,** 3705–3720 (2013).
72. Lee, S. & Makris, N. C. The array invariant. *J. Acoust. Soc. Am.* **119,** 336–351 (2006).
73. Gong, Z., Ratilal, P. & Makris, N. C. Simultaneous localization of multiple broadband non-impulsive acoustic sources in an ocean waveguide using the array invariant. *J. Acoust. Soc. Am.* **138,** 2649–2667 (2015).
74. Tran, D., Andrews, M. & Ratilal, P. Probability distribution for energy of saturated broadband ocean acoustic transmission: results from Gulf of Maine 2006 experiment. *J. Acoust. Soc. Am.* **132,** 3659–3672 (2012).
75. Jain, A., Ignisca, A., Yi, D., Ratilal, P. & Makris, N. Feasibility of ocean acoustic waveguide remote sensing (OAWRS) of Atlantic cod with seafloor scattering limitations. Remote Sens. **6,** 180–208 (2014).
76. Jagannathan, S., Kusel, E., Ratilal, P. & Makris, N. Scattering from extended targets in range-dependent fluctuating ocean-waveguides with clutter from theory and experiments. *J. Acoust. Soc. Am.* **132,** 680–693 (2012).
77. Andrews, M., Chen, T. & Ratilal, P. Empirical dependence of acoustic transmission scintillation statistics on bandwidth, frequency and range in New Jersey continental shelf. *J. Acoust. Soc. Am.* **125,** 111–124 (2009).
78. Collins, M. D. Generalization of the split-step Padé solution. *J. Acoust. Soc. Am.* **93,** 1736–1742 (1983).
79. Ainslie, M. A. Neglect of bandwidth of Odontocetes echo location clicks biases propagation loss and single hydrophone population estimates. *J. Acoust. Soc. Am.* **134,** 3506–3512 (2013).
80. Makris, N. C. The effect of saturated transmission scintillation on ocean-acoustic intensity measurements. *J. Acoust. Soc. Am.* **100,** 769–783 (1996).
81. Bertsatos, I., Zanolin, M., Chen, T. R., Ratilal, P. & Makris, N. C. General second order covariance of Gaussian maximum likelihood estimate applied to passive source localization in a fluctuating ocean waveguide. *J. Acoust. Soc. Am.* **128,** 2635–2651 (2010).
82. Thode, A. *et al.* Necessary conditions for a maximum likelihood estimate to become asymptotically unbiased and attain the Cramer-Rao lower bound Part II: range and depth localization of a sound source in an ocean waveguide. *J. Acoust. Soc. Am.* **112,** 1890–1910 (2002).
83. Andrews, M., Gong, Z. & Ratilal, P. Effects of multiple scattering, attenuation and dispersion in waveguide sensing of fish. *J. Acoust. Soc. Am.* **130,** 1253–1271 (2011).
84. DiFranco, J. V. & Rubin, W. L. *Radar Detection (Artech House, 1980).*
85. Bergmann, P. G., Yaspan, A., Gerjuoy, E., Major, J. K. & Wildt, R. *Physics of Sound in the Sea* (Gordon and Breach, 1968).
86. Urick, R. J. *Principles of Underwater Sound* 29–65 and 343–366 (McGraw Hill, 1983).
87. Širović, A., Hildebrand, J. A. & Wiggins, S. M. Blue and fin whale call source levels and propagation range in Southern Ocean. *J. Acoust. Soc. Am.* **122,** 1208–1215 (2007).
88. Weirathmueller, M. J., Wilcock, W. S. & Soule, D. C. Source levels of fin whale 20 Hz pulses measured in the Northeast Pacific Ocean. *J. Acoust. Soc. Am.* **133,** 741–749 (2013).
89. Newhall, A. E., Lin, Y. T., Lynch, J. F., Baumgartner, M. F. & Gawarkiewicz, G. G. Long distance passive localization of vocalizing sei whales using an acoustic normal mode approach. *J. Acoust. Soc. Am.* **131,** 1814–1825 (2012).
90. Jensen, F. B., Kuperman, W. A., Porter, M. B. & Schmidt, H. *Computational Ocean Acoustics* 708–713 (Springer-Verlag, 2011).
91. Clay, C. S. & Medwin, H. *Acoustical Oceanography* 494–501 (John Wiley, 1977).
92. Burdic, W. S. *Underwater Acoustic System Analysis* 322–360 (Prentice-Hall, 1984).
93. Küsel E. T. *et al.* Cetacean population density estimation from single fixed sensors using passive acoustics. *J. Acoust. Soc. Am.* **129,** 3610–3622 (1983).
94. Marques, T. A., Thomas, L., Ward, J., DiMarzio, N. & Tyack, P. L. Estimating cetacean population density using fixed passive acoustic sensors: an example with Blainvilles beaked whales. *J. Acoust. Soc. Am.* **125,** 1982–1994 (2009).
95. Barlow, J. & Taylor, B. L. Estimates of sperm whale abundance in the northeastern temperate Pacific from a combined acoustic and visual survey. *Mar. Mamm. Sci.* **21,** 429–445 (2005).
96. Martin, S. W. *et al.* Estimating minke whale (*Balaenoptera acutorostrata*) boing sound density using passive acoustic sensors. *Mar. Mamm. Sci.* **29,** 142–158 (2013).
97. Marques, T. A., Munger, L., Thomas, L., Wiggins, S. & Hildebrand, J. A. Estimating North Pacific right whale *Eubalaena japonica* density using passive acoustic cue counting. Endanger. *Species Res.* **13,** 163–172 (2011).
98. Marques, T. A. *et al.* Estimating animal population density using passive acoustics. *Biol. Rev. Camb. Philos. Soc.* **88,** 287–309 (2013).
99. Battista, T. A., Clark, R. D. & Pittman, S. An ecological characterization of the Stellwagen Bank national marine sanctuary region: oceanographic, biogeographic, and contaminants assessment. US Department of Commerce, National Oceanic and Atmospheric Administration, National Ocean Service, Center for Coastal Monitoring and Assessment, 265282 (2006).
100. Stark, H. & Woods, J. *Probability, Statistics, and Random Processes for Engineers* (Prentice Hall, 2011).

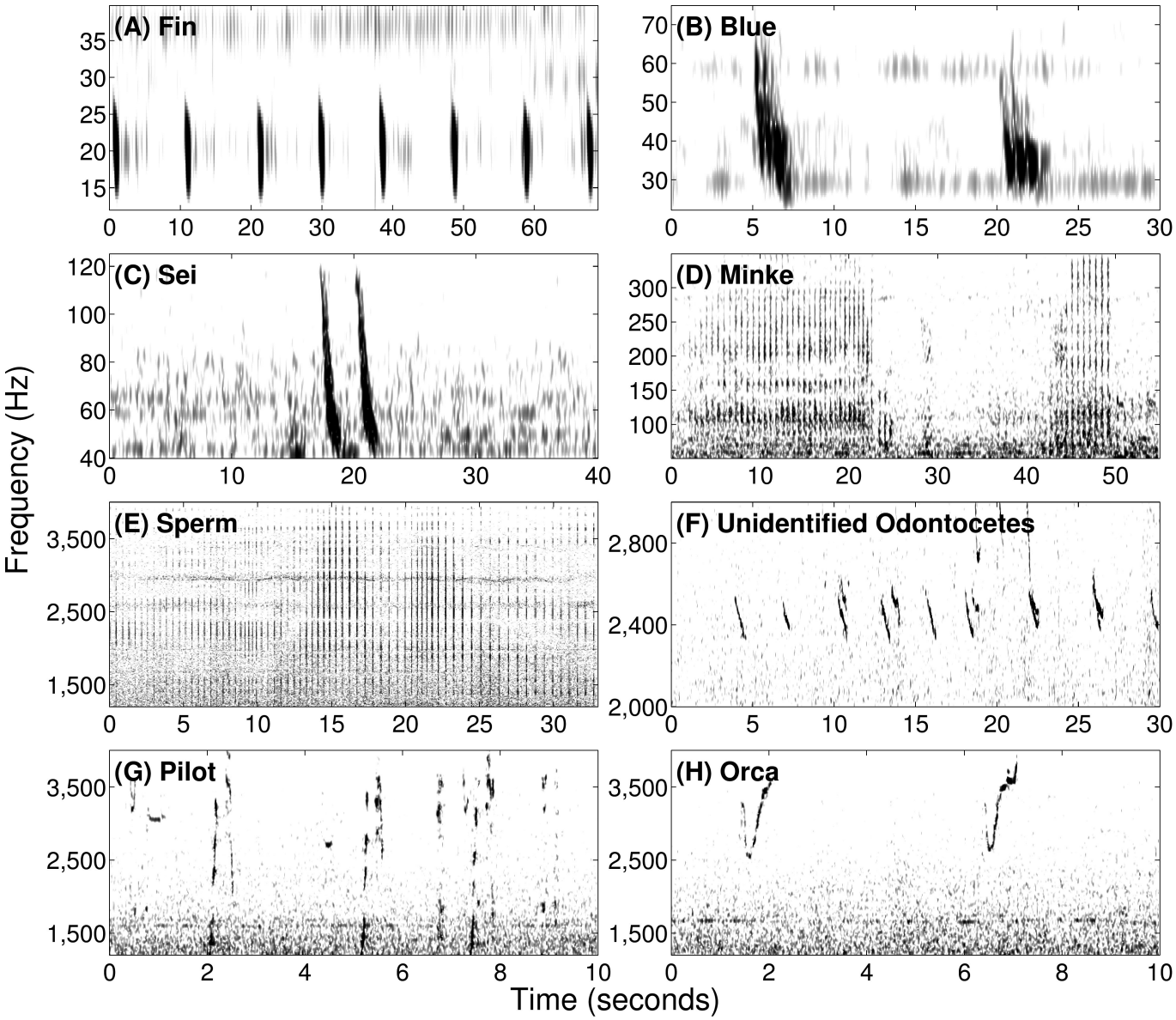

Extended Data Figure 1 | Spectrograms of MM vocalizations. a–h, Beamformed spectrograms of typical repetitive vocalizations from diverse MM species observed using the POAWRS receiver array in the Gulf of Maine from 19 September to 6 October 2006.

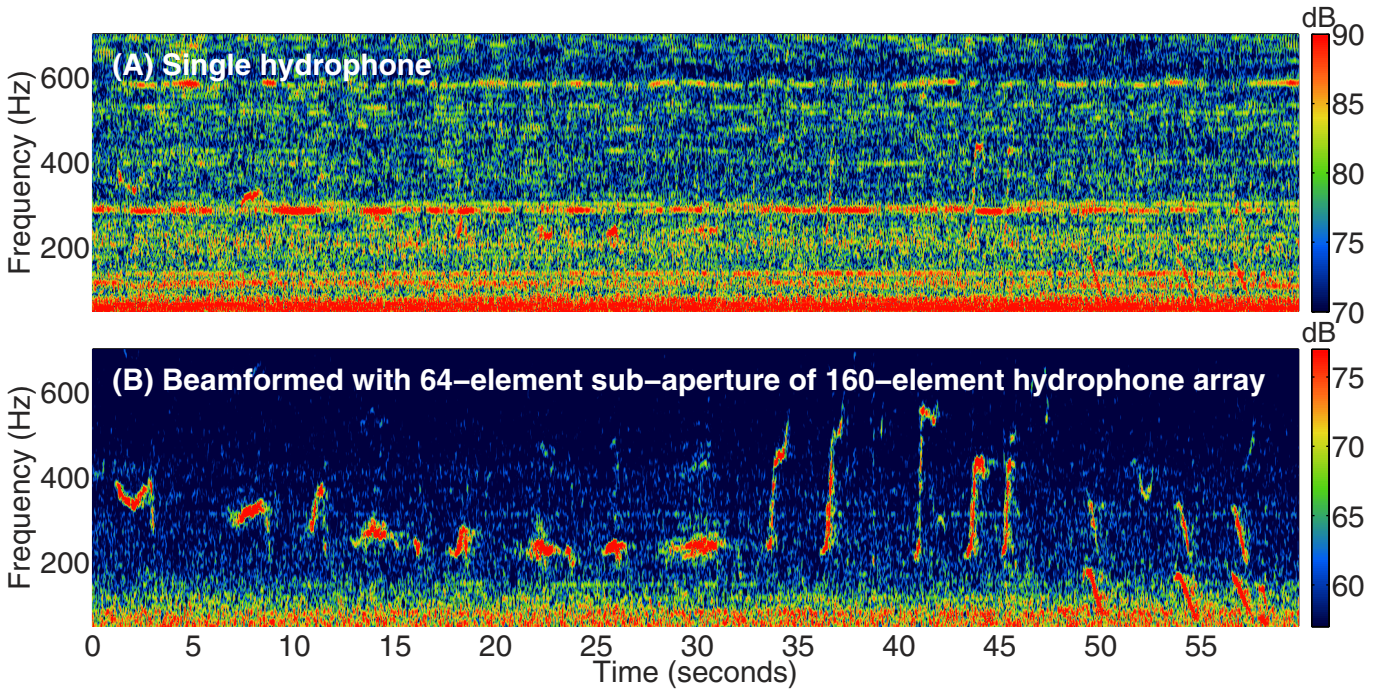

Extended Data Figure 2 | Coherent array processing enhances SNR. **a**, **b**, Compare single hydrophone measured spectrogram (**a**) with spectrogram after coherent beamforming (**b**) with 64-element sub-aperture of POAWRS 160-element hydrophone array. The song vocalization from a humpback individual roughly 35 km away from the POAWRS receiver array recorded on 2 October 2006 at 23:48:45 EDT is enhanced by 18 dB above the background noise after beamforming in **b** where whale bearing is −64.16° from array broadside.

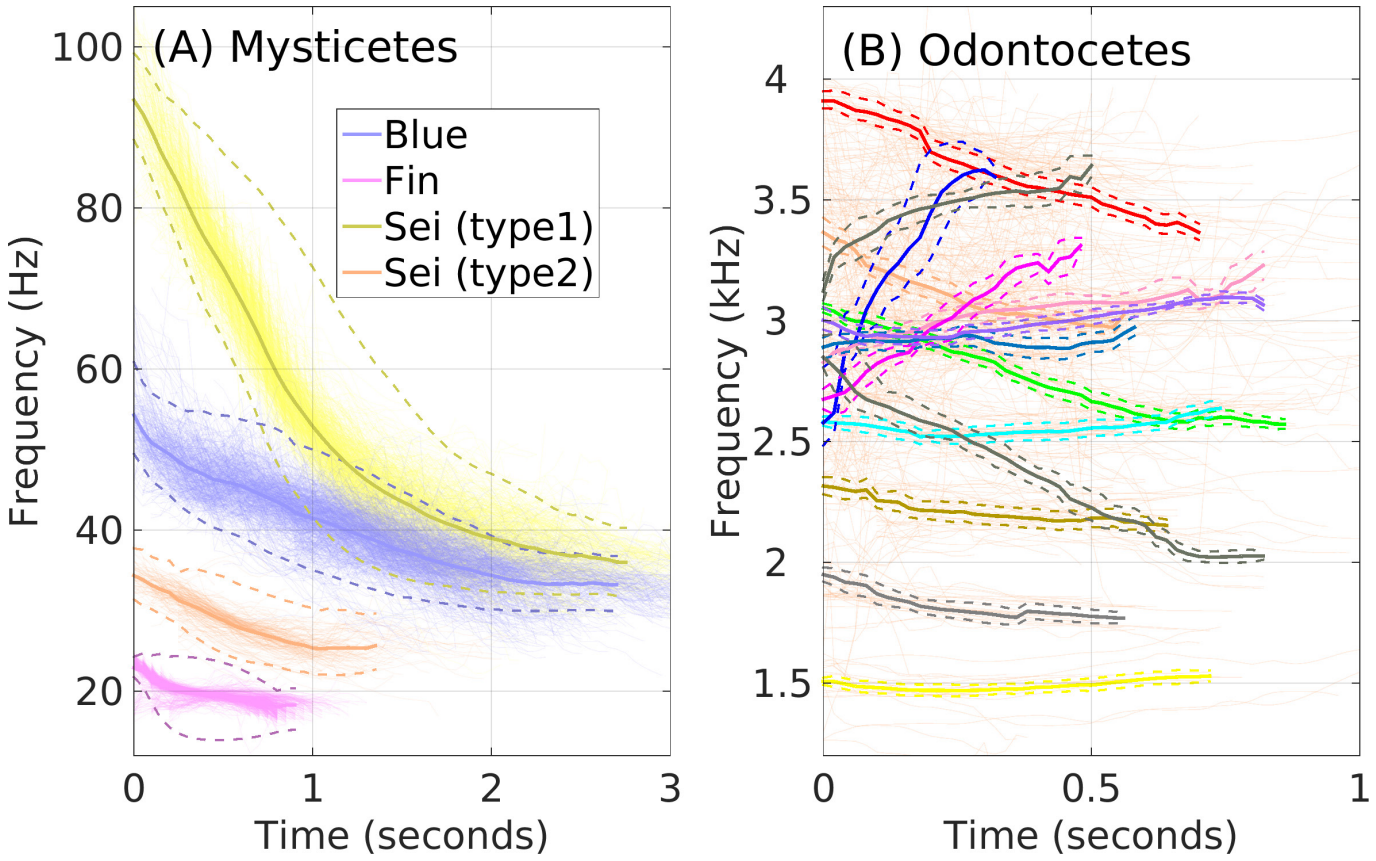

Extended Data Figure 3 | Pitch-tracks of baleen and toothed whales. **a**, Pitch-tracks of repetitive mysticete vocalizations in the 10 to 100 Hz range. Thick solid curves are the means of roughly 500 to 1,000 vocalizations of each type. Mean instantaneous bandwidth of the pitch-tracks are indicated by the dashed curve. Even though blue and sei type I calls have some overlapping bandwidth, they can be well separated using the upper frequency f_U and slope $df/d\tau$ features (Extended Data Table 2). **b**, Mean pitch-track and instantaneous bandwidth of repetitive odontocete downsweep vocalizations in the 1 to 4 kHz range.

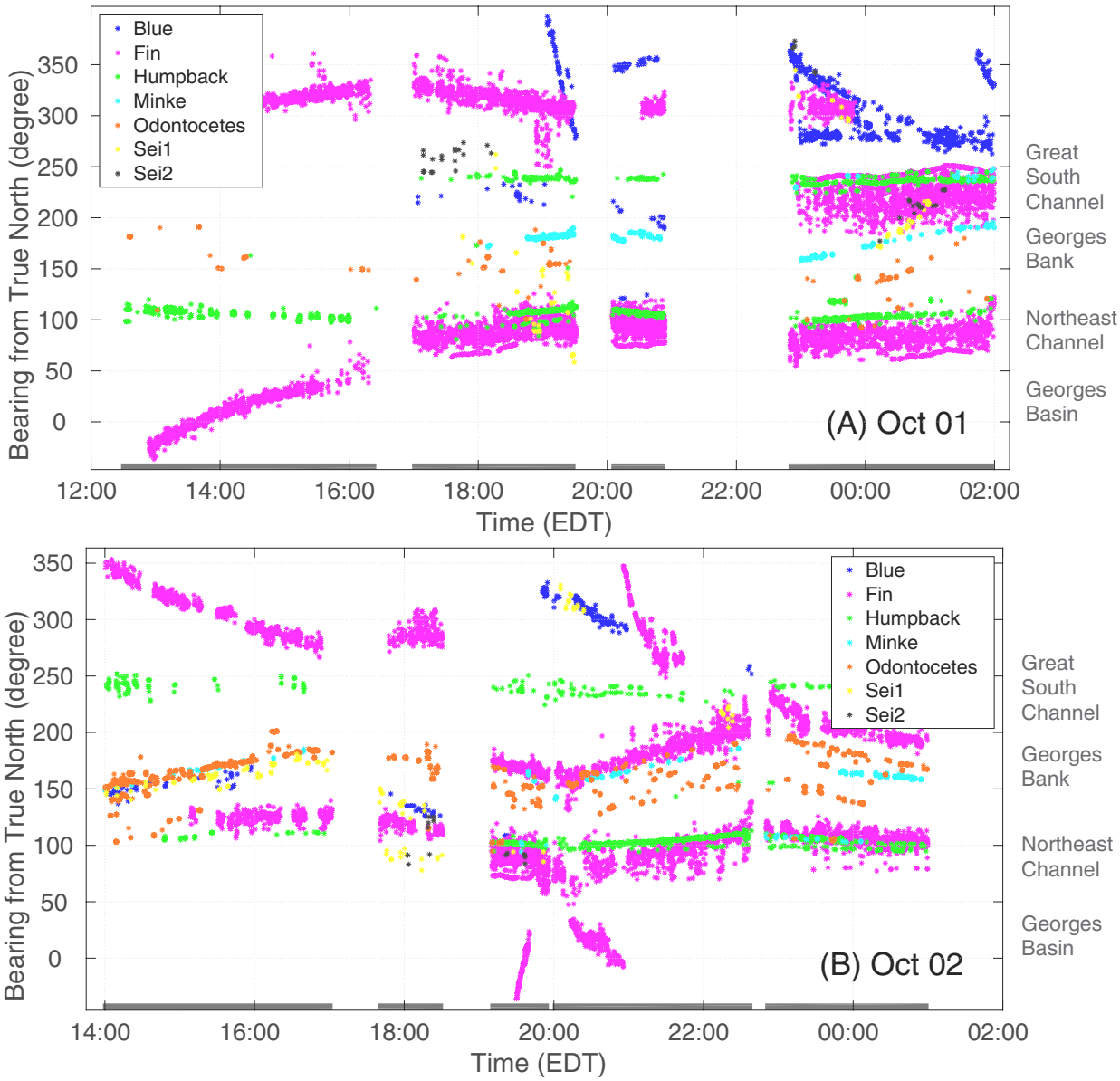

Extended Data Figure 4 | Daily POAWRS measured MM vocalization bearings. a, **b**, MM vocalization bearings from diverse species measured by POAWRS receiver array on 1 October 2006 (**a**) and 2 October 2006 (**b**). The bearings are measured from true North in clockwise direction with respect to the instantaneous spatial locations of the receiver array centre. The techniques used here for resolving source bearing ambiguity about the horizontal line-array axis are provided in Methods section 3. The shaded bars on the *x* axis indicate the operation time periods of the receiver array.

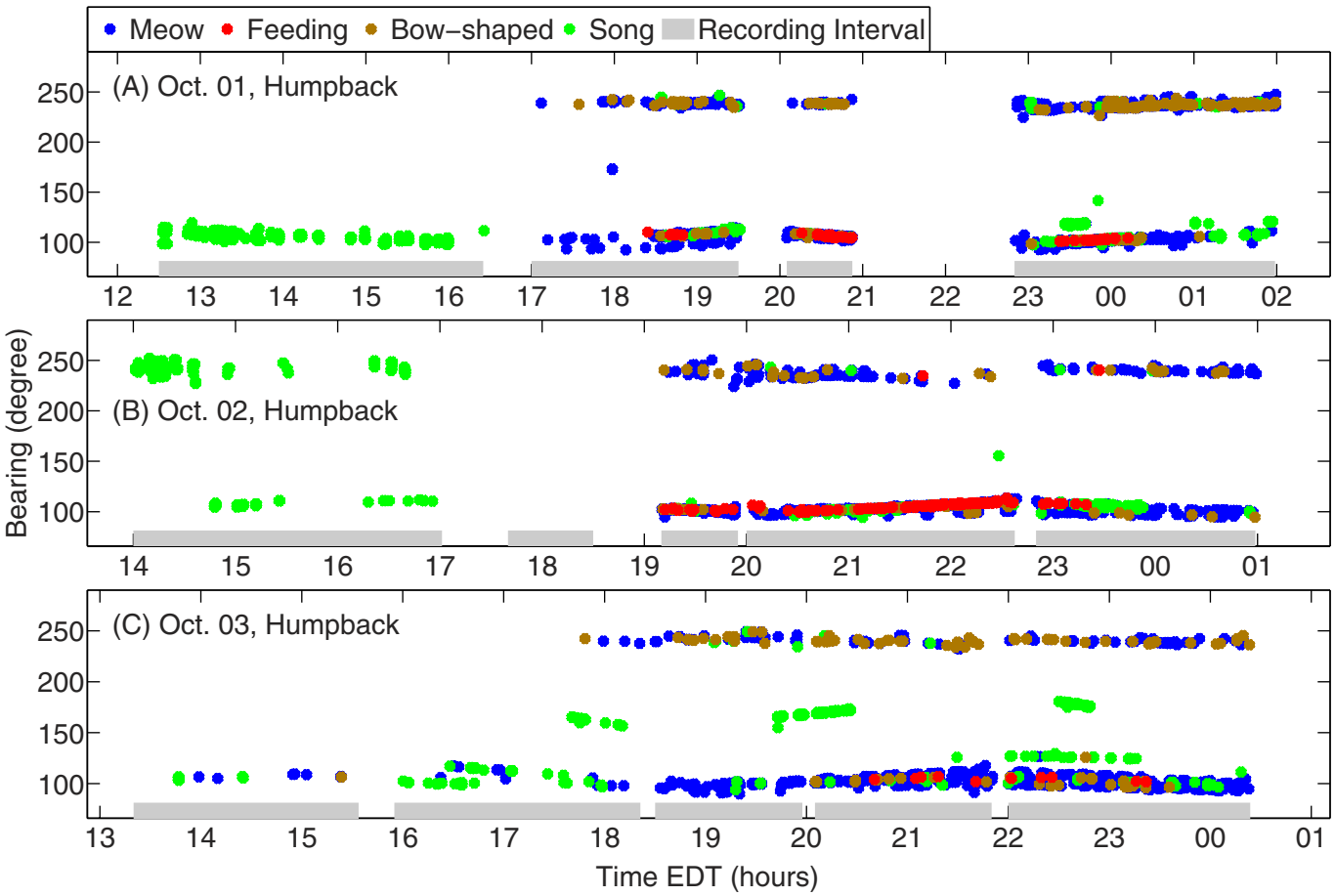

Extended Data Figure 5 | Daily humpback vocalization repertoire. a–c, Bearings and repertoire of humpback vocalizations measured by POAWRS receiver array on 1 October 2006 (**a**), 2 October 2006 (**b**), and 3 October 2006 (**c**). The 'meow', 'bow', and 'feeding' call characteristics are provided in ref. 7.

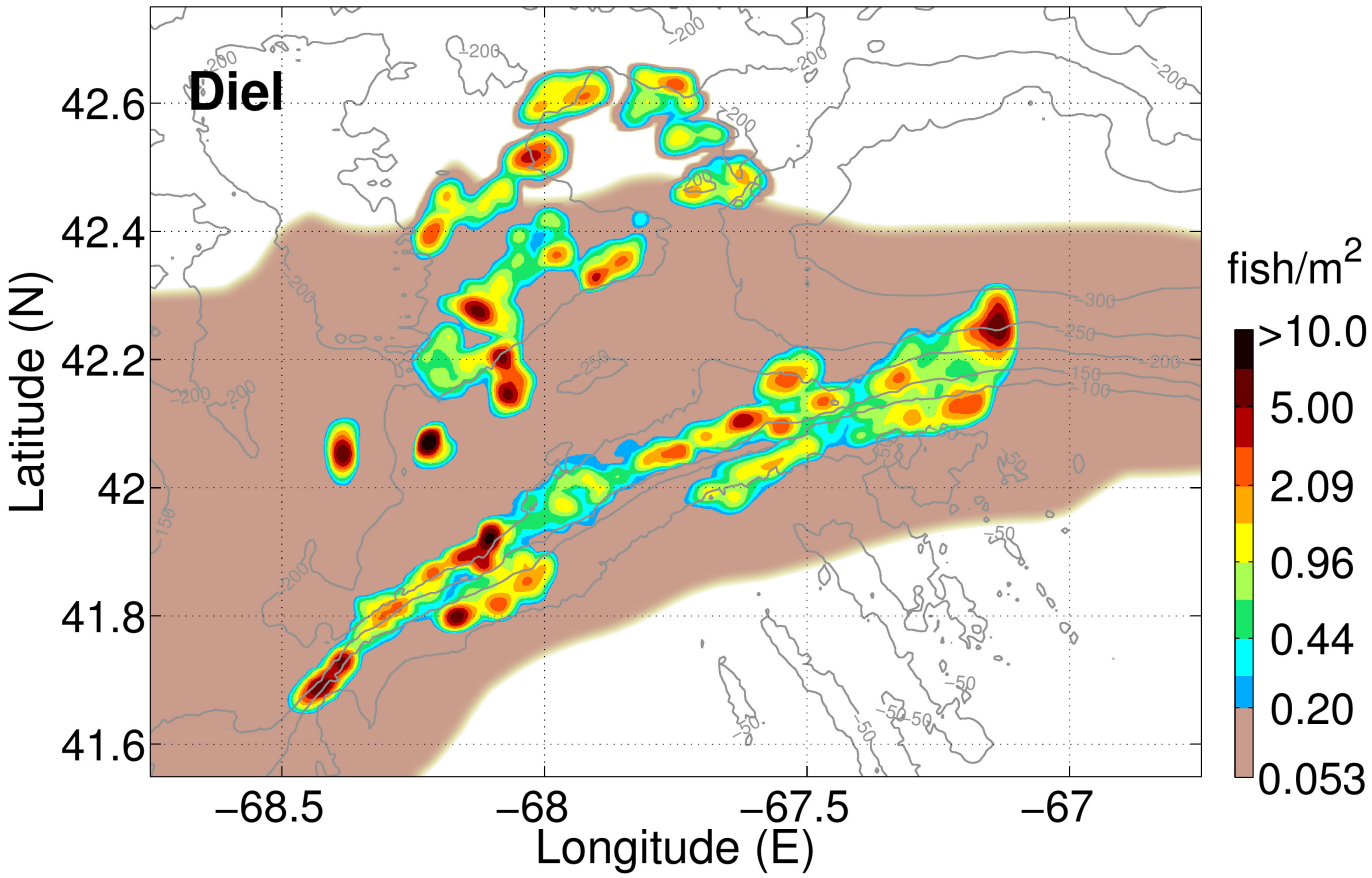

Extended Data Figure 6 | Diel Atlantic herring shoaling areal population densities. Measured herring shoaling areal population densities (ranging from 0.2 fish per m^2 to over 10 fish per m^2) determined from OAWRS[12,13] survey in the Gulf of Maine from 26 September 2006 to 6 October 2006, upon calibration with tens of thousands of coincident and co-located conventional ultrasonic fisheries echosounding measurements, combined with trawl sampling for identity and biological–physiological characterization of fish populations[15,16]. The mean diffuse herring density of 0.053 fish per m^2 is determined from conventional ultrasonic fisheries echosounding. The bathymetric data (contours shown in grey) were obtained from the US National Centers for Environmental Information.

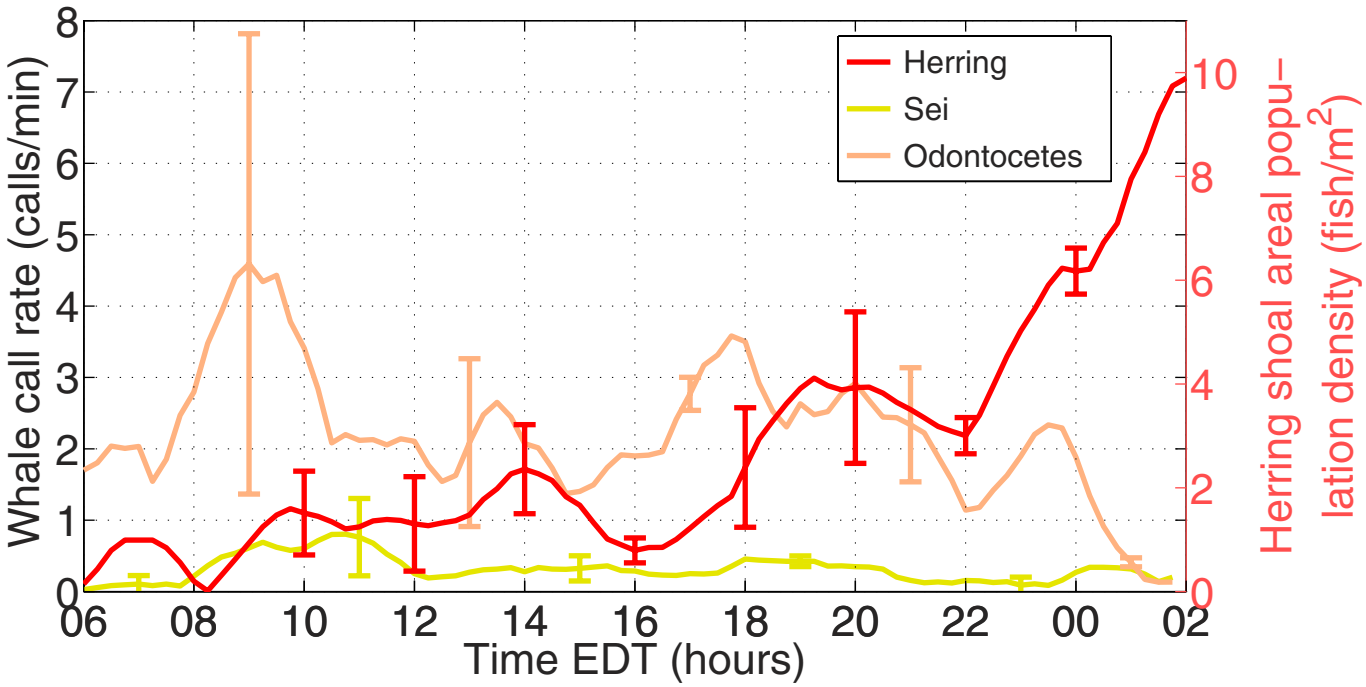

Extended Data Figure 7 | Diel MM call rate and herring shoal areal population density time series. Mean diel call rates for sei whales and odontocetes in general are not correlated to the diel Atlantic herring shoal mean areal population density. The error bars indicate standard deviations obtained from averaging the time series over multiple diel cycles from 26 September 2006 to 6 October 2006. The period from roughly 2–6 EDT contains a data gap.

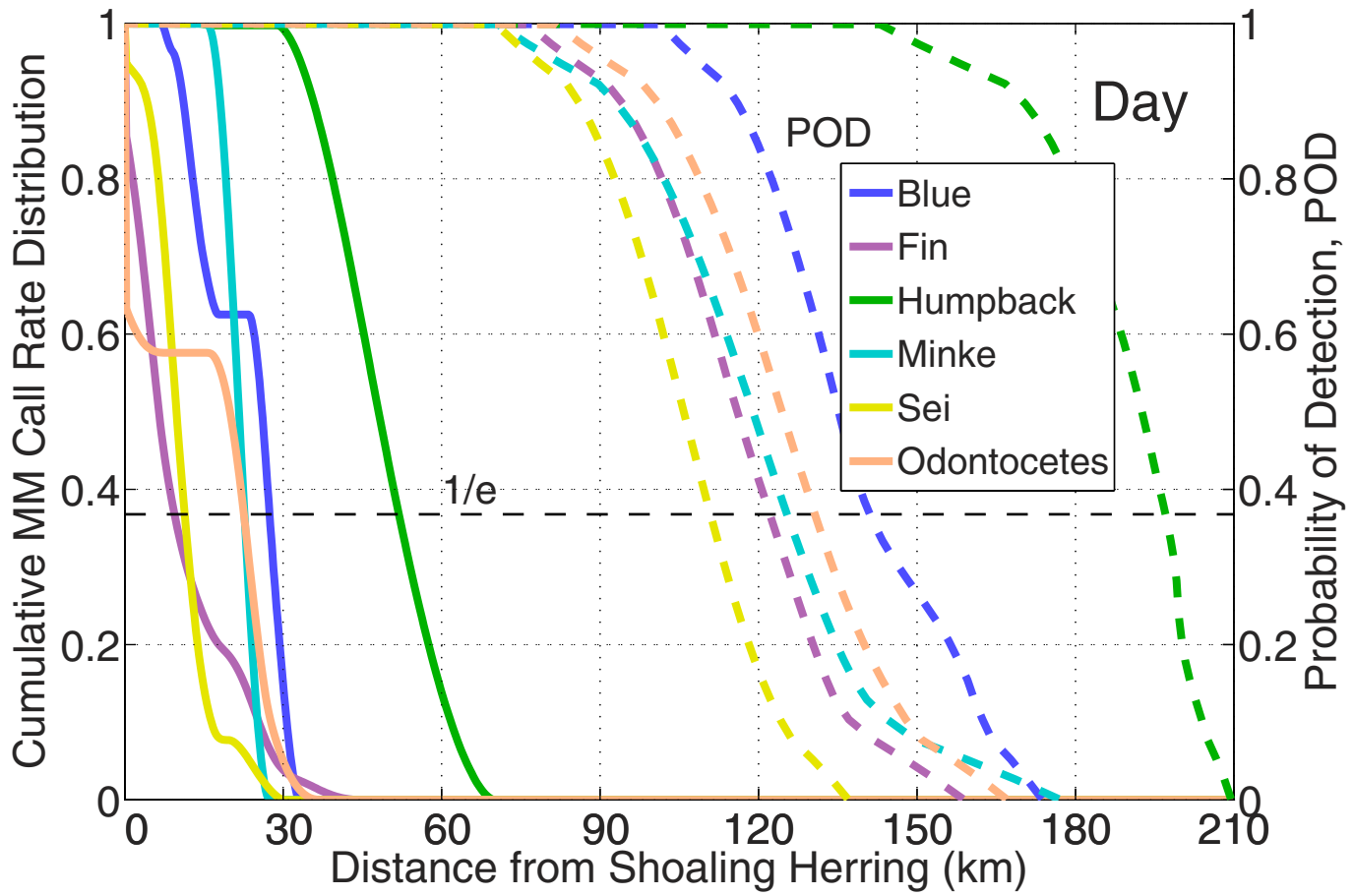

Extended Data Figure 8 | Cumulative diurnal MM call rate distribution. Cumulative diurnal MM vocalization rate distribution and azimuthally-averaged POAWRS MM POD as a function of minimum distance from diurnal herring shoaling areas. The *e*-folding distances of the cumulative MM vocalization rate distributions decrease from day (shown here) to night (in Fig. 3b) by 27.3 to 7 km (blue), 9.3 to 3.9 km (fin), 51.7 to 3.5 km (humpback), 22.5 to 0 km (minke), 11.2 to 8.1 km (sei), and 22.4 to 5.5 km (odontocetes). The percentage of vocalizations that fully overlap with herring shoaling areas increase from day to night by 0% to 18% (blue), 14% to 40% (fin), 6% to 44% (humpback), 0% to 71% (minke), and 5% to 24% (sei), but decrease by 36% to 29% (odontocetes).

Extended Data Table 1 | MM species daily call rate and temporal correlations

MM species	C_{MM} calls/day	$\frac{C_{MM,\text{night}}}{C_{MM,\text{day}}}$	$r_{MM,fish}$	$r_{MM_I,MM_{II}}$					
				blue	fin	humpback	minke	sei	odontocetes
blue	470	10	0.91	1	0.67	0.78	0.48	-0.17	-0.46
fin	14,000	2.5	0.82	0.67	1	0.85	0.79	0.02	-0.27
humpback	2,000	10	0.87	0.78	0.85	1	0.84	-0.29	-0.30
minke	690	5	0.64	0.48	0.79	0.84	1	-0.18	-0.20
sei	440	0.77	-0.11	-0.17	0.02	-0.29	-0.18	1	0.44
odontocetes	3200	0.83	-0.42	-0.46	-0.27	-0.30	-0.20	0.44	1

The temporal correlation $r_{MM,fish}$ of MM vocalization rate time series to fish shoaling areal population density time series, as well as the temporal correlation $r_{MMI, MMII}$ between distinct MM species vocalization rate time series over the diel cycle are calculated using Methods equations (1) and (2) respectively.

Extended Data Table 2 | Large baleen whale repetitive vocalization pitch-track features

Characteristics	fin	blue	sei (type 1)	sei (type 2)
f_L (Hz)	13.7 ± 0.6	28 ± 3	32 ± 6	22 ± 3
f_U (Hz)	24.9 ± 1	56 ± 8	88 ± 12	36 ± 4
$\overline{f}$ (Hz)	19.8 ± 0.4	40 ± 4	50 ± 7	28 ± 3
$\overline{B}$ (Hz)	8 ± 1	12.5 ± 4	21 ± 5	8.1 ± 1.5
$\overline{B}/\overline{f}$	0.40 ± 0.05	0.31 ± 0.08	0.4 ± 0.1	0.29 ± 0.06
τ (s)	0.8 ± 0.2	2 ± 0.5	2 ± 0.5	1 ± 0.3
$\frac{df}{d\tau}$ (Hz/s)	-4.6 ± 2	-9 ± 5	-24 $\pm$ 10	-6.6 ± 3
$\frac{d^2f}{d\tau^2}$ (Hz/s^2)	2.5 ± 9	0.5 ± 6	13 ± 8	5.6 ± 8

Vocalization characteristics in the 10 to 100 Hz range from large baleen whales detected with POAWRS receiver array in the Gulf of Maine in autumn 2006. The characteristics are the lower f_L, upper f_U, and mean $\overline{f}$ frequencies, mean instantaneous bandwidth B, relative instantaneous bandwidth $B/\overline{f}$ duration τ, slope $df/d\tau$, and curvature $d^2f/d\tau^2$. The slope and curvature are obtained from second order nonlinear curve-fit to the vocalization traces obtained via pitch-tracking.

doi:10.1038/nature16960

I. Probability of detection for MM vocalizations from diverse species with POAWRS receiver array. Here we formulate and quantify the probability of detection (POD) $P_D(r)$ of the MM vocalizations from each species as a function of range r from the POAWRS receiver array shown in Fig. 3, Extended Data Fig. 8, and Supplementary Information Fig. 1 below.

For a MM located at range r from the POAWRS receiver array, its vocalization signal can be detected above the ambient noise if the sonar equation[7,86,90–92] is satisfied,

$$NL + DT - AG < L_S - TL(r), \tag{1}$$

where L_S is the MM vocalization source level, NL is the ambient noise level in the frequency band of the MM vocalization signal, AG is the coherent beamforming gain of our passive receiver array, DT is the detection threshold, and TL is the broadband transmission loss. We use a calibrated[13,74–77] parabolic equation based Range-dependent Acoustic propagation Model (RAM)[78] to calculate the broadband transmission loss[13,74–77,79] via $TL = 10\log_{10}(\int_{f_L}^{f_U} Q(f)\langle|G(r|r_0,f)|^2\rangle df)$, where $G(\mathbf{r}|\mathbf{r_0},f)$ is the waveguide Green function for MM source located at $\mathbf{r_0}$ and receiver at $\mathbf{r}$, $Q(f)$ is the normalized MM vocalization spectra, and f_L and f_U are the lower and upper frequencies of the analysis. The model takes into account the environmental parameters, such as the range-dependent bathymetry, seafloor geo-acoustic properties[13], MM source and POAWRS receiver array location, and over 200 experimentally measured water-column sound speed profiles (Fig. 3 of Ref. [13]) to stochastically[80–82] compute the propagated acoustic intensities via Monte-Carlo simulation using the approach outlined in Refs. [13,75–77,83]. The stochastic broadband transmission loss model calculations have been extensively calibrated and verified with (1) thousands of one-way transmission loss measurements made during the same GOM 2006 experiment discussed here at the same time and at the same location[13,74]; (2) thousands of two-way transmission loss measurements made

from herring shoal returns and verified by conventional fish finding sonar and ground truth trawl surveys during the same GOM 2006 experiment discussed here at the same time and at the same location[12,13,16]; (3) roughly one hundred two-way transmission loss measurements made from calibrated targets with known scattering properties during the same GOM 2006 experiment discussed here at the same time and at the same location[76]; and (4) thousands of one-way transmission loss measurements made during a past OAWRS experiment conducted in a similar continental shelf environment[77].

The MM vocalizations are detected from the beamformed spectrograms and typically occupy roughly M number of independent time-frequency pixels $\Delta f \Delta t$ where M varies between 3 to 24 depending on the species. We first calculate the detection probability $p_{D,1}(r)$ in a single frequency-time pixel using,[84,86]

$$p_{D,1}(r) = \int_{-\infty}^{+\infty} f_{L_R}(L_R(r)) \int_{-\infty}^{L_R(r)-DT} f_{L_N}(L_N) dL_N dL_R, \tag{2}$$

where $f_{L_N}(L_N)$ is the probability density function of the log-transformed ambient noise pressure-squared $L_N(t,f) = 10\log_{10}(|P_N(t,f)/P_{ref}|^2) = S_N(t,f) + 10\log_{10}(\Delta f) - AG$ within a single beamformed spectrogram time-frequency pixel in the frequency range of the MM vocalization, where $P_N(t,f)$ is the noise pressure at time t within frequency bin Δf centered at frequency f and $S_N(t,f)$ is the omnidirectional ambient noise spectral density level; $f_{L_R}(L_R(r))$ is the probability density function of the received MM vocalization signal log-transformed pressure-squared $L_R(r|t,f) = 10\log_{10}(|P_R(r|t,f)/P_{ref}|^2) = L_S - TL(r) + 10\log_{10}\frac{\Delta f}{B(t)}$ within a single beamformed spectrogram time-frequency pixel, where $P_R(r|t,f)$ is the received MM vocalization signal pressure, and $B(t)$ is the instantaneous bandwidth of that signal at time t. The number of independent beamformed spectrogram frequency-time pixels occupied by the MM vocalization signal is related to the instantaneous bandwidth via $M\Delta f \Delta t = \tau B(t)$, where τ is the signal du-

ration. An exponential-Gamma distribution[74,80,85] describes the log-transformed ambient noise pressure-squared and log-transformed received MM vocalization pressure-squared within a single beamformed spectrogram time-frequency pixel,

$$f_{L_N}(L_N) = \frac{1}{(10\log_{10} e)\Gamma(\mu)}\Big(\frac{\mu}{\langle P_N^2\rangle}\Big)^{\mu} 10^{\mu L_N/10}\exp(-\mu\frac{10^{L_N/10}}{\langle P_N^2\rangle}) \tag{3}$$

$$f_{L_R}(L_R(r)) = \frac{1}{(10\log_{10} e)\Gamma(\mu)}\Big(\frac{\mu}{\langle P_R^2(r)\rangle}\Big)^{\mu} 10^{\mu L_R(r)/10}\exp(-\mu\frac{10^{L_R(r)/10}}{\langle P_R^2(r)\rangle}), \tag{4}$$

where μ is the time-bandwidth product or number of statistically independent fluctuations of the respective pressure-squared quantities. Since the beamformed spectrograms have time-frequency pixels that satisfy $\Delta f \Delta t = 1$, both the ambient noise level and the received MM vocalization signal level within each beamformed spectrogram time-frequency pixel can be treated as instantaneous with time-bandwidth product $\mu = 1$ and 5.6 dB standard deviation. For the received MM vocalization signal level, this standard deviation includes both the standard deviation of the MM vocalization source level, as well as the standard deviation of the broadband waveguide transmission loss. The 5.6 dB standard deviation used here for the received MM vocalization signal level is consistent with the standard deviation shown for the measured humpback song unit statistical distribution in Fig. 17 of Ref. [7].

We assume the received MM vocalization signal is detectable if it stands above the ambient noise in at least 30% of the M time-frequency pixels of the beamformed spectrogram. The overall probability of detection, $P_D(r)$, for the MM vocalizations from each species as a function of range r from the POAWRS receiver array is then calculated from the Gaussian approximation to the binomial cummulative distribution function (CDF)[84] as,

$$P_D(r) = 1 - \Phi\Big(\frac{0.3M - Mp_{D,1}(r)}{\sqrt{Mp_{D,1}(r)(1-p_{D,1}(r))}}\Big). \tag{5}$$

where $\Phi(z) = \frac{1}{\sqrt{2\pi}}\int_{-\infty}^{z} e^{-u^2/2}du$, and shown in Supplementary Information Fig. 1. The Gaussian approximation to the binomial CDF is an appropriate model for the overall performance of the

detector when considering the thousands of MM vocalizations analyzed. The exponential-Gamma distribution[74,80] for the log-transform of Gaussian field measurements, used here to model the probability density function of the received MM vocalization level and the ambient noise level, has been calibrated with (1) thousands of log-transformed intensity measurements from controlled source transmissions made during the same 2006 Gulf of Maine experiment discussed here at the same time and at the same location[74], and (2) thousands of measurements made during a past OAWRS experiment conducted in a similar continental shelf environment[77].

The MM vocalization source levels L_s used here are estimated from a subset of the POAWRS received vocalizations, in units of dB re 1 μPa at 1m, and are given by 189 ± 5.6 for blue and fin, 180 ± 5.6 for humpback, 179 ± 5.6 for sei, 179 ± 5.6 for minke, and 165 ± 5.6 for the odontocete downsweep chirp signals. The MM vocalization source levels estimated here are an average over one or several vocalization types detected by the POAWRS system, depending on the species, as described in Methods section 2. The vocalization source level estimates here are consistent with previous estimates for blue and fin[87,88], humpback[7], and sei[89]. The omnidirectional ambient noise spectral density levels $S_N(f)$ are estimated directly from the POAWRS receiver array using data segments that are devoid of MM vococalizations. The $S_N(f)$ (in units of dB re 1 μPa^2/Hz) are roughly 80 ± 5.6 for fin, 76 ± 5.6 for blue and sei, 69 ± 5.6 for minke, 64 ± 5.6 for humpback, and 50 ± 5.6 for odontocetes.

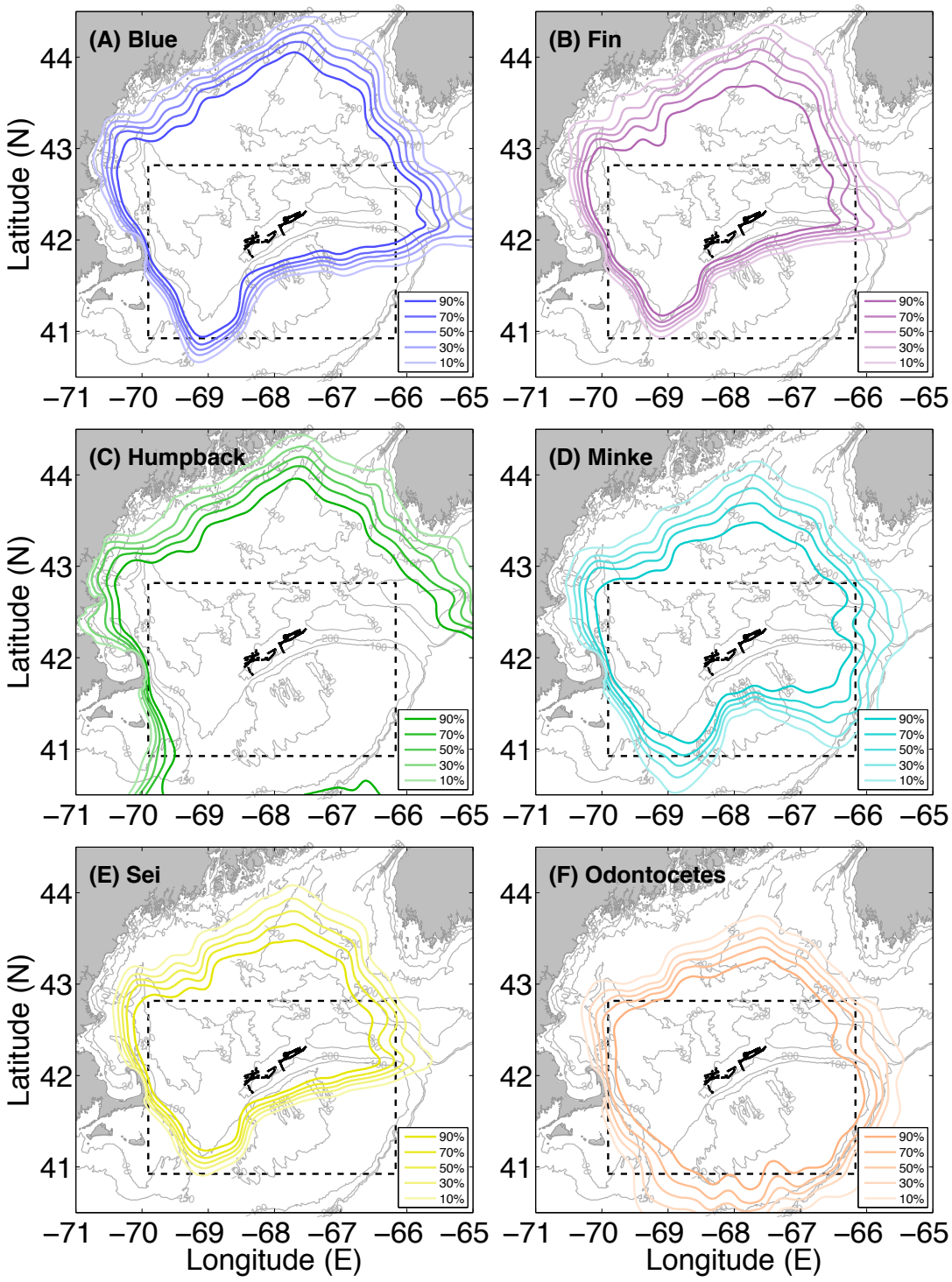

Supplementary Information Figure 1 | The azimuthally-dependent POAWRS MM vocalization probability of detection contours for diverse species. The vast majority of MM vocaliza-

tions in Figs. 1 and 2 originate in areas where the POAWRS receiver array has greater than 0.9 probability of detection. The bathymetric data (contours shown in gray) are obtained from the U.S. National Centers for Environmental Information.

II. POAWRS and OAWRS sampling of annually occuring Fall season MM foraging and fish spawning activity on the northern flank of Georges Bank. The POAWRS system sampled at 8,000 samples per second over roughly 10-16 hours each day for 13 days over 64 directions, which leads to over 200 billion independent time sampling points. This large data set shows sequences of correlated spatial events over thousands of square kilometers where no whale vocalizations are present in bounded regions, versus sequences of correlated spatial events over thousands of square kilometers where vocalizations are present, consistently over thousands of independent temporal snapshots of the POAWRS survey region, as seen in Figs. 1-4 and Extended Data Figs. 1-8. Such a large sequence of correlated events has a negligligbly small probability of being a false positive result due to random fluctuation. When this finding of correlated spatial segmentation is combined with the large body of existing measurements that: (1) herring are observed to consistently spawn on the Northern Flank of Georges Bank each fall over many decades[9,12–16,32–34]; (2) whales (humpback, fin, sei, minke and various odontocetes) are consistently observed visually to migrate and feed on spawning herring during their spawning period in various parts of the world[9,18,24,28,29,34,57,101–105]; (3) the seasonal high population density regions visually observed over decades[10,99] for the same whale species of this study are consistent with those of the high resolution, wide-area POAWRS findings of this study; the correlated space-time behavior that we observed between whales and herring is expected to be highly repeatable annually in the fall, and the probability that it is not highly repeatable is expected to be negligibly small.

III. MM diel, diurnal, and nocturnal spatial vocalization rate distributions. The vocal MMs are found to be concentrated in species-specific population centers with varying degrees of spatial overlap that can vary over the diel cycle depending on the species (see Figs. 1-2 and Supplementary Information Figs. 2, 3 and 4). The fins occupy a central location with high vocal activity concentrated on north-central Georges Bank and west of Georges Basin areas. The humpacks flank the fin distribution on both sides with partial overlap and vocal activity concentrated primarily on northeastern Georges Bank, and a lesser concentration spread over Franklin Basin to the Great South Channel. The densest concentration of blue vocalizations partially overlap with those of fin between Georges and Rodgers Basins. The minkes maintain relatively high vocal activity on north-central Georges Bank throughout the diel cycle, partially overlapping with densest fin concentrations at night. The densest sei vocalization concentrations occur during the day between Georges and Rodgers Basins. The odontocetes are distributed over the entire northern Georges Bank with several hotspots in the eastern, central and western sectors. Note that the units for the humpback whale call rate density distribution shown in Figs. 1-3 and 13 of Ref. [7] is a typographical error and should be (# calls)/[(min)(5nmi)^2].

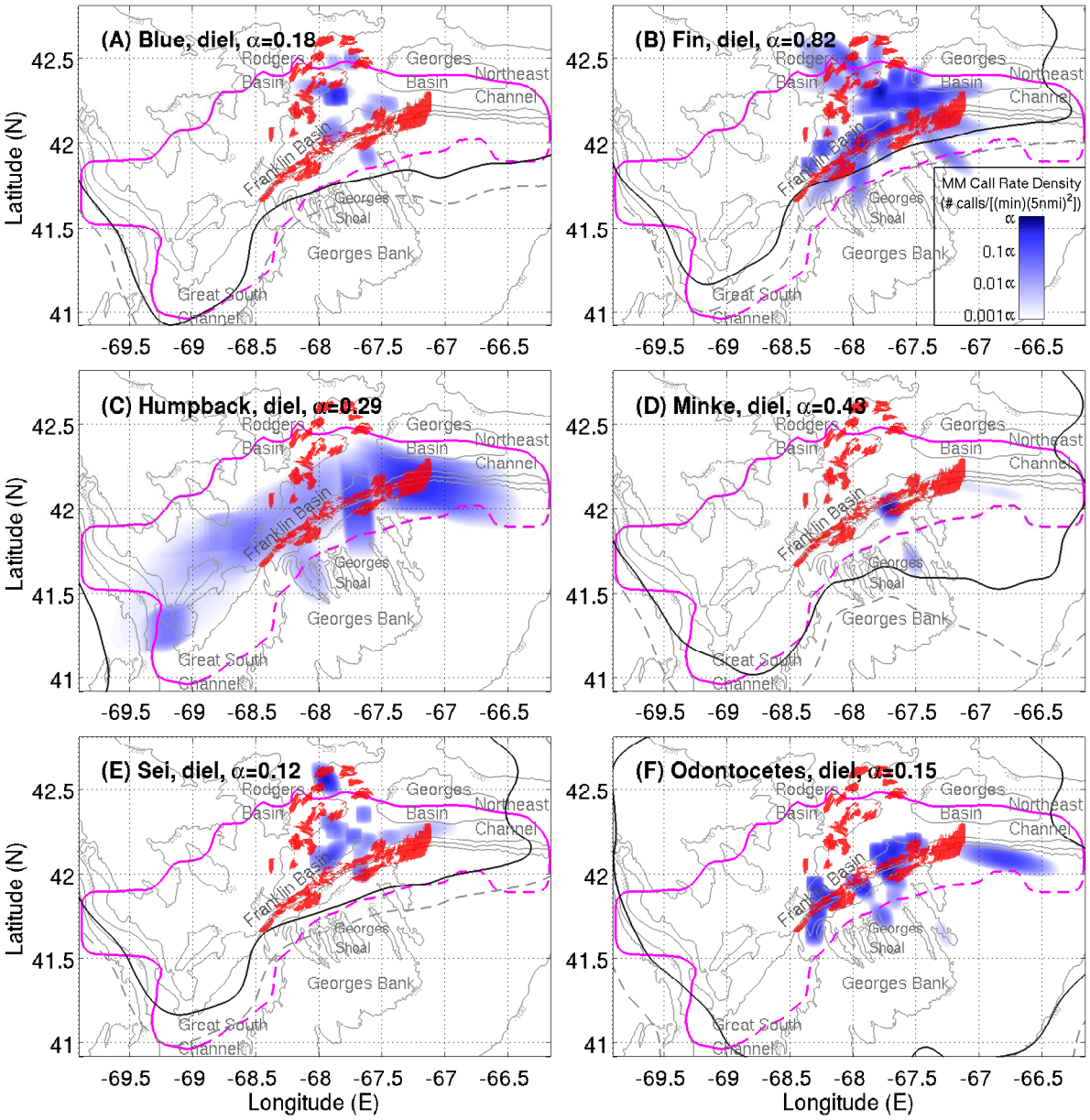

Supplementary Information Figure 2 | Full diel cycle vocalization rate spatial distribution of diverse MM species overlain with spawning herring distribution. Dense herring shoals (> 0.2 fish/m^2, red shaded areas) imaged using OAWRS system[12,13] and diffuse herring populations (~ 0.053 fish/m^2, bounded by magenta line) obtained from conventional fish finding sonar[15,16]. The modelled POAWRS MM vocalization 0.8 POD (solid black) and 0.2 POD (dashed gray) contours are indicated for each species. The bathymetric data (contours shown in gray) are obtained from the U.S. National Centers for Environmental Information.

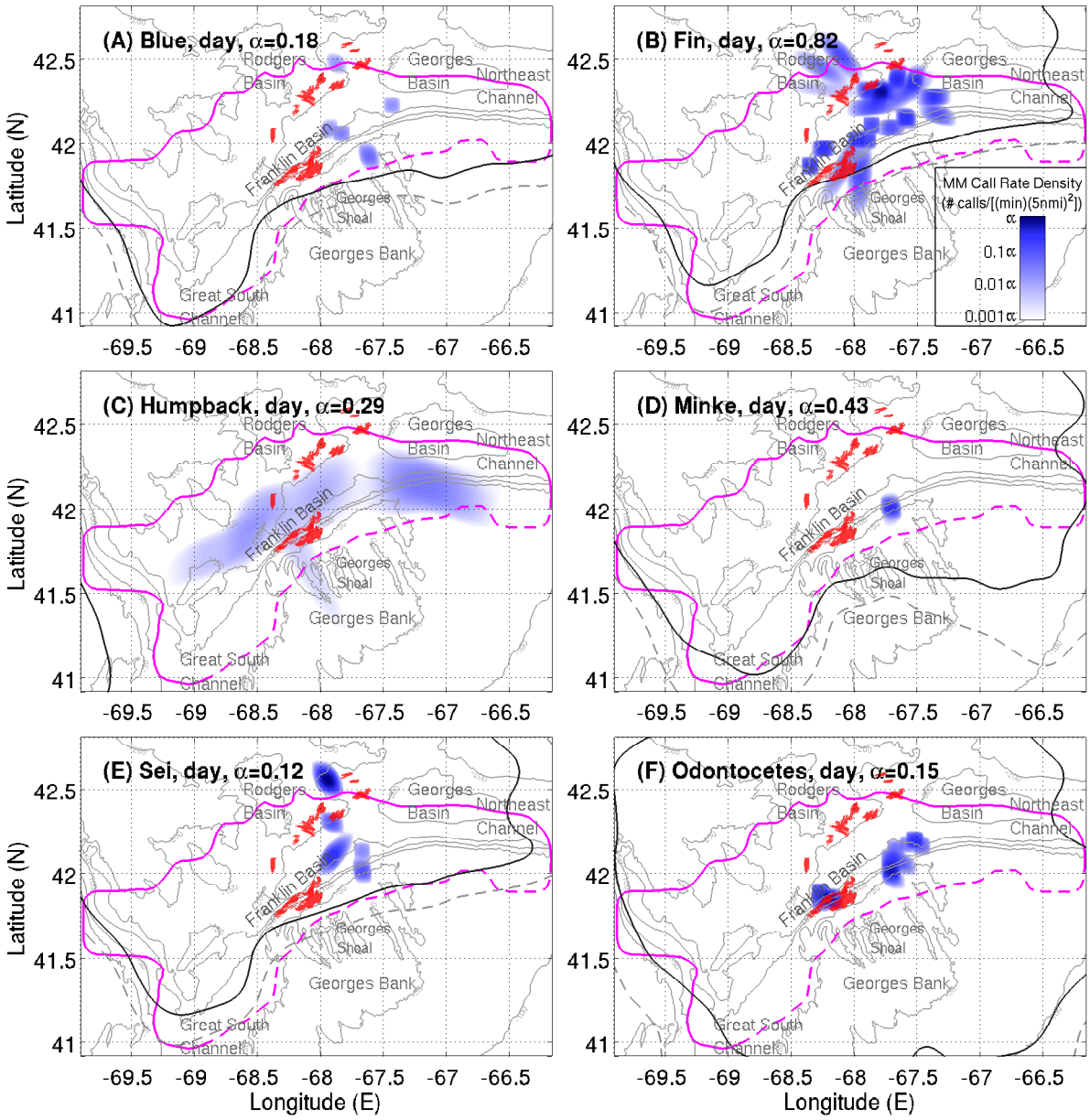

Supplementary Information Figure 3 | Diurnal vocalization rate spatial distribution of diverse MM species overlain with diurnal herring populations. Dense herring shoals (> 0.2 fish/m^2, red shaed areas)[12,13], and diffuse herring populations (~ 0.053 fish/m^2, bounded by magenta line)[15,16] are shown. The modelled POAWRS MM vocalization 0.8 POD (solid black) and 0.2 POD (dashed gray) contours are indicated for each species. The bathymetric data (contours shown in gray) are obtained from the U.S. National Centers for Environmental Information.

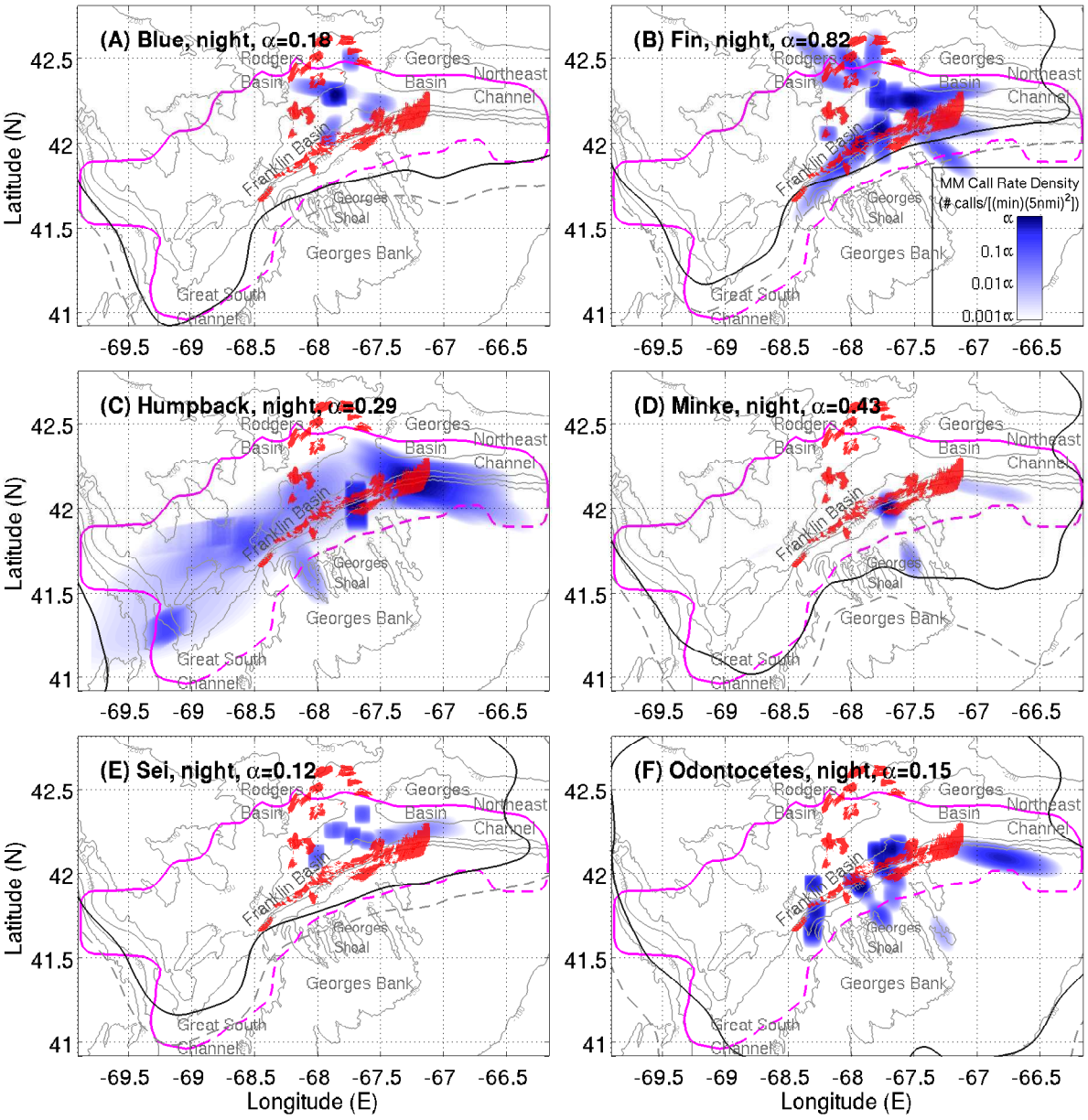

Supplementary Information Figure 4 | Nocturnal vocalization rate spatial distribution of diverse MM species overlain with nocturnal herring populations. Dense herring shoals ($>$ 0.2 fish/m^2, red shaed areas)[12,13], and diffuse herring populations ($\sim$ 0.053 fish/m^2, bounded by magenta line)[15,16] are shown. The modelled POAWRS MM vocalization 0.8 POD (solid black) and 0.2 POD (dashed gray) contours are indicated for each species. The bathymetric data (contours shown in gray) are obtained from the U.S. National Centers for Environmental Information.

In regions where the probability of detection (POD) is lower due to unfavorable transmission, the POAWRS system will have a lower probability of detecting vocalizing MMs. Similarly, when the POD is high due to favorable transmission and no detections are made, there is high confidence that no vocalizing MMs are present. For humpbacks, odontocedes and minkes, the 100% to 80% POD region extends well to the north and south of the region where call rates are detected for these species by 40 km to over 100 km, and by at least 10-20 km for seis and blues. This gives confidence to the findings quantified in Fig. 3(B) that the call rates for these species originate primarily in the vicinity of dense herring shoals. For fins, the 100%-80% POD region extends more than 80 km to the north of where calls are detected. To the south, however, a small fraction of fin calls (6%) are detected in areas where the probability of detection due to unfavorable transmission is lower than 80%. The POD-normalized fin diel call rate spatial distribution shown in Extended Data Fig. 5(B) is almost identical to that in Extended Data Fig. 2(B) without the POD normalizations, except for the southern-most tips of the fin call rate spatial distribution where the call rate densities are enhanced by a factor of roughly 1.5 from POD normalizations, i.e. call rate density divided by POD at a given location. The MM call rate spatial distributions obtained here are consistent with historical distributions which show very low occurrence for all baleen whale species in central and southern Georges Bank based on 30 years of visual surveys (see Fig. 5.3.8 of Ref. [99]). These overall findings are also consistent with year round visual surveys of MMs in the US northeastern continental shelf, including the Georges Bank region, from 1980 to 1983 which found large baleen whales concentrated in areas where the mean water depth[106] ranged from 91 m to 147 m. A poor transmission environment for a given MM species is suboptimal for the acoustic communications of that species and may be less favored by the species. The shallow waters of central Georges Bank are also dangerous for ships as well as large MMs due to the presence of highly variable sand bars which vary with weather conditions and so may be less favored. In other parts of the worlds ocean,

such as the Gulf of California[107], the Antarctic Seas[108] and the Mediteranean Seas[109], fins whales are found concentrated in water depths much deeper than 100 m.

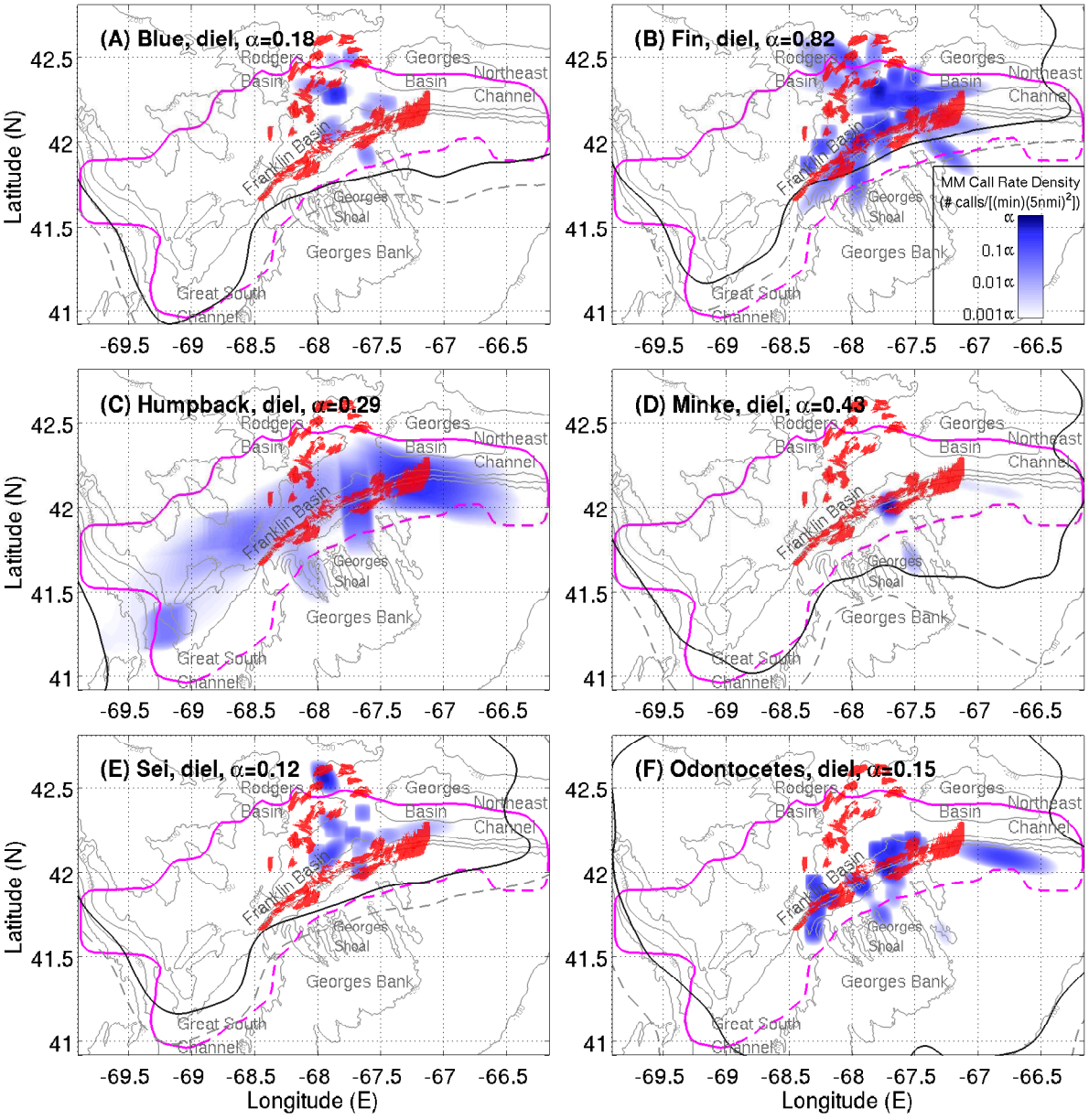

Supplementary Information Figure 5 | POD-normalized full diel cycle vocalization rate spatial distribution of diverse MM species. The POD-normalized diel MM vocalization rate spatial distributions for diverse species are similar to those without POD normalizations shown in Supplementary Information Fig. 2. All other contours and overlays shown here are identical to those in Supplementary Information Fig. 2. The bathymetric data (contours shown in gray) are obtained

from the U.S. National Centers for Environmental Information.

IV. Consistency between MM acoustic cue production rate and areal population density. Historical Fall season visual surveys (1970-2005) of MMs in the Gulf of Maine[99,106] are consistent with the overall volume of calls measured each day by the POAWRS receiver array for each species after accounting for the acoustic cue production rate per individual of each species, which is also found to be consistent with previous measurements[42–45,57,88,110]. This visual data can be used to infer the areal population density of MMs which, in units of abundance per 1000 km^2 in their densest region shown in Fig. 1, is expected to range from 25 to 50 for humpbacks, 10 to 22 for fins, 4 to 16 for minkes, and 3 to 24 for seis[52]. For pilot whales, their population density is expected to exceed 243 per 1000 km^2. The overall population density for delphinids is expected to exceed 540 per 1000 km^2.

The historical sightings per unit effort (SPUE, in units of abundance per 1000 km of survey track) values provided for the Fall season hotspot areas on northern Georges Bank in Ref. [99] for each species were converted to areal population density n_A after accounting for the perpendicular sighting distances[111,112] expected for each species via $n_A = \frac{SPUE}{1000\times 2\mu}1000$. Here μ is the effective[113,114] perpendicular sighting distance or effective strip half-width[30,111] obtained from a rectangular approximation to the perpendicular sighting distance distribution, and estimated to be $\mu \approx 1.6$ km for large, $\mu \approx 1.25$ km for medium, and $\mu \approx 0.6$ km for small cetaceans respectively, taking an average of the effective strip half-widths reported in Refs. [106,115,116] determined from line-transect sighting surveys. The areal population density estimates for various MM species obtained here are within the range reported in Ref. [106] for the Georges Bank region in the Fall season based on visual observations over years 1980-1983. Since these estimates are dependent on

the perpendicular sighting distances, which can vary with sea state, weather condition, experience level of the visual observer and observation deck height[106,116], and potentially have other unquantified sources of uncertainty, they are rough approximations that are expected to vary by *at least* a factor of 2 given the factor of 1/2 to 2 variation reported in measured perpendicular sighting distances (see Table 11 of Ref. [106]). More accurate wide-area MM population density estimates can be obtained with the POAWRS system when coincident visual observations or coincident data from acoustically tagged whales are combined in the analysis.

Even if a combined areal population density of fins and humpbacks is a factor of 7 to 15 times smaller than the areal population density of the delphinids, these large baleen whales can have significant consumption impact, consistent with the proposition[9] that fins and humpbacks are the dominant MM consumers. This is because a single large baleen whale can engulf several hundred to a few thousand herring in one gulp via filter feeding, while a delphinid generally consumes a single fish with its teeth at any given time[28,29]. As can be noted from Extended Data Table 1, fins and humpbacks in close vicinity to herring shoals together account for over 70% of the total volume of MM vocalizations recorded by POAWRS at frequencies of up to 4 kHz, which is consistent with a significant role in herring consumption.

Given the population density estimate, we can estimate the mean acoustic cue production rate per individual of each species (Supplementary Information Table 1). These mean call rates per individual lie within the span observed for fin[42–45,88] and humpback[57,110] when both the vocal and non-vocal MMs that were observed are included in the averaging. (No prior results found for sei and minke.)

V. Zooplankton distribution. Plankton samples from the Gulf of Maine[117–120] were collected at various stations with a 61 cm diameter circular bongo frame fitted with a net of 0.333 mm mesh. The gear was towed obliquely at 1.5 knots to a maximum depth of 200 m or 5 m from the bottom and back to the surface, which ever was less. A flowmeter was suspended in the centre of the bongo frame to measure the volume of water filtered during the tow. Specimens were preserved in 5% formalin. Samples were reduced to approximately 500 organisms by subsampling with a modified box splitter in the laboratory. Zooplankton were sorted, counted, and identified to the lowest possible taxa at the Polish Plankton Sorting Centre in Szczecin, Poland. Abundance is expressed as number per m^3. The results from 249 samples from stations approximately 2-40 km apart acquired in the time period from Jul 01 to Oct 31, 2006[117–119] are considered here.

The Fall season Sep.–Oct. 2006 total zooplankton abundance measurements for the area shown in Figs. 1-2 have a mean volumetric density of roughly 715± 550 /m^3, which include *Centropages typicus* (200±190 /m^3), *Centropages hamatus* (130±350 /m^3), *Paracalanus parvus* (90±70 /m^3), siphonophores (50±140 /m^3), *Calanus finmarchicus* (35±55 /m^3), and euphausids (13±37 /m^3) (see Supplementary Information Fig. 6). This range of total zooplankton densities are typical for the fall season in this area, a factor of roughly three to eight times smaller than those occuring in the summer months[117,118] of Jul.-Aug. 2006, which had a mean of roughly 2200± 2250 /m^3 in 2006. The Sep.–Oct. 2006 total zooplankton volumetric densities are equivalent those found in areas where baleen whales are less likely to feed on zooplankton. The total zooplankton densities found in baleen whale zooplankton-feeding areas[20,21,121–124] are significantly higher, and typically range from 4,000/m^3 to over 10,000/m^3.

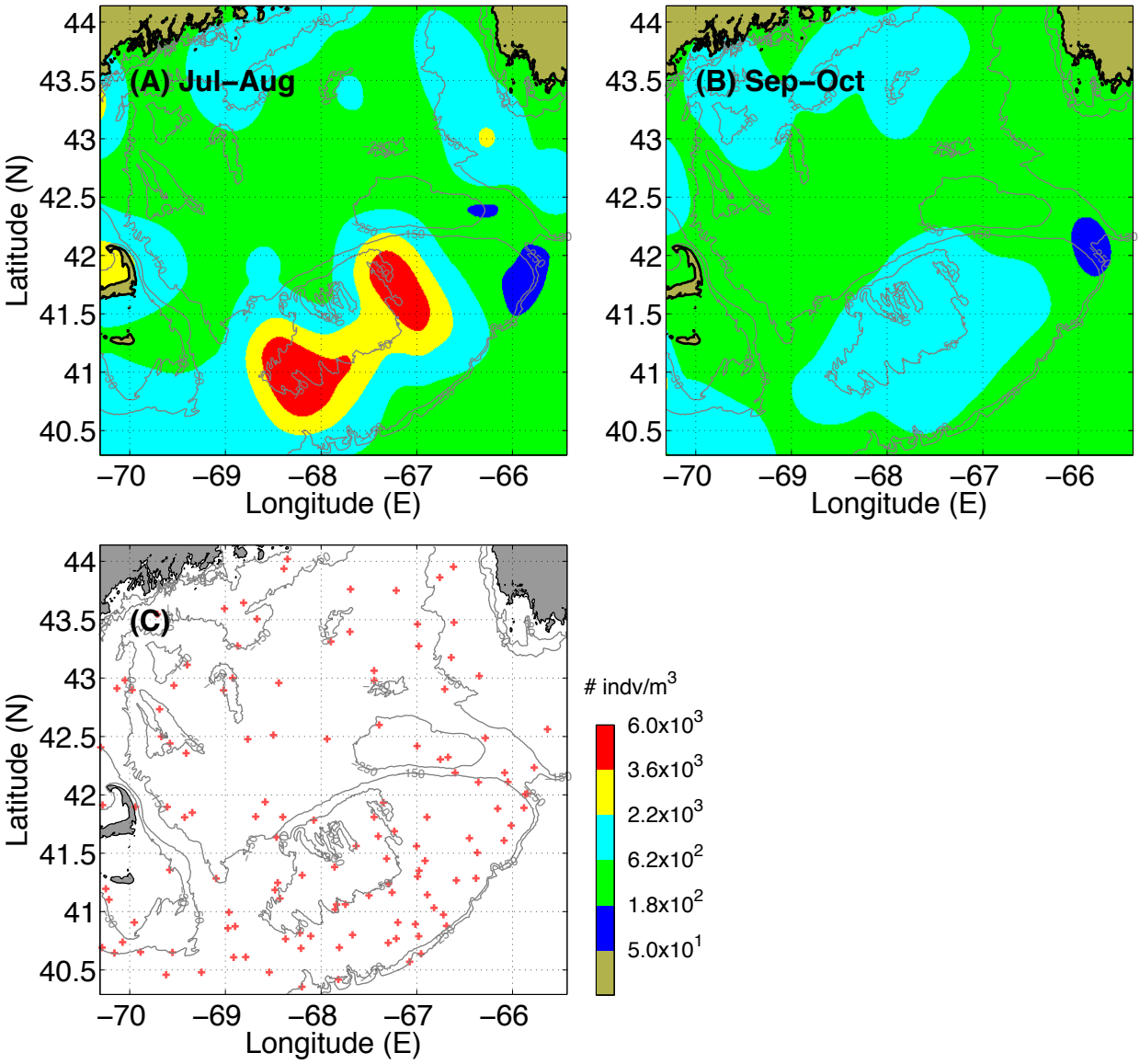

Supplementary Information Figure 6 | Measured total zooplankton volumetric density. Zooplankton density in units of abundance/m^3 are shown for (A) July-August and (B) September-October 2006 time frames from bongo net sampling at locations[117–119] indicated by the plus symbol in (C). The bathymetric data (contours shown in gray) are obtained from the U.S. National Centers for Environmental Information.

MM species	$c_{MM,total,peak}$ (calls/min)	$c_{MM,ind}$ (calls/min per individual)
fin	14.2 ± 2	0.55 – 1.6
humpback	3.6± 0.6	0.06 – 0.2
minke	1.4± 0.6	0.05 – 0.5
sei	0.8± 0.7	0.004 – 0.5

Supplementary Information Table 1 | MM population and individual call rates POAWRS-measured peak call rates $c_{MM,total,peak}$ (from Fig. 4 and Extended Data Fig. 7), and estimated mean individual acoustic cue production rates $c_{MM,ind}$ for diverse MM species. For minkes, their call rates refer to the number of 5 second duration buzz sequences expected per minute.

References

The citations 1-100 refer to the References in the main article and Methods section. The citations 101-124 refer to References included here.

101. Lindstrøm, U., Haug, T. & Rttingen, I. Predation on herring, Clupea harengus, by minke whales, Balaenoptera acutorostrata, in the Barents Sea. *ICES J. of Marine Science: Journal du Conseil*, **59**, 58-70 (2002).

102. Woodley, T. H. & Gaskin, D. E. (1996). Environmental characteristics of North Atlantic right and fin whale habitat in the lower Bay of Fundy, Canada. *Canadian J. of Zoology*, **74** 75-84 (1996).

103. Simon, M., Wahlberg, M., Ugarte, F. & Miller, L. A. Acoustic characteristics of underwater tail slaps used by Norwegian and Icelandic killer whales (Orcinus orca) to debilitate herring (Clupea harengus). *J. of Experimental Bio.* **208**, 2459-2466 (2005).

104. Gibbons, J. Capella, J. J. & Valladares, C. Rediscovery of a humpback whale, Megaptera novaeangliae, feeding ground in the Straits of Magellan, Chile. *J. Cetacean Research and Management* **5**, 203-208 (2003).

105. Bowen, W. D. Role of marine mammals in aquatic ecosystems. *Mar. Ecol. Prog. Ser.* **158**, 267-274 (1997).

106. Payne, P. M., Selzer, L. A. & Knowlton, A. R. Distribution and density of cetaceans, marine turtles, and seabirds in the shelf waters of the northeast U. S., June 1980 - Dec. 1983, based on shipboard observations. National Marine Fisheries Service, Woods Hole. NA81FAC00023: 245.

107. Gallo-Reynoso, J. P., Bean, T. L., Palomino, E., Figueroa-Carranza, A. L. & Ortiz, L. 18. Mysticetes on the midriff area of the Gulf of California during the summers of 1995, 1996 and 1997. In *Contribuciones mastozoolgicas en homenaje a Bernardo Villa*, Ed. by V. Sanchez-Cordero & R. A. Medellin, 205-213, Mexico: Instituto de Biologia e Instituto de Ecologia. UNAM. (2005).

108. Williams, R., Hedley, S. L. and Hammond, P. S. Modeling distribution and abundance of Antarctic baleen whales using ships of opportunity. *Ecology and Society* **11**, 1 (2006).

109. Notarbartolo-Di-Sciara, G., Zanardelli, M., Jahoda, M., Panigada, S. & Airoldi, S. The fin whale Balaenoptera physalus (L. 1758) in the Mediterranean Sea. *Mammal Review* **33**, 105-150 (2003).

110. Silber, G. K. The relationship of social vocalizations to surface behavior and aggression in the Hawaiian humpback whale *(Megaptera novaeangliae). Canadian Journal of Zoology* **64**, 2075-2080 (1986).

111. Borchers, D. L., Buckland, S. T. & Zucchini, W. Estimating animal abundance: closed populations. Springer (2002)

112. Moore, S. E., Waite, J. M., Mazzuca, L. L., & Hobbs, R. C. Mysticete whale abundance and observations on prey association on the central Bering Sea shelf. *J. of Cetacean Research and Management* **2**, 227-234 (2000).

113. Mandel, L. & Wolf, E. Optical coherence and quantum optics. Cambridge university press (1995).

114. Middleton, D. & Institute of Electrical and Electronics Engineers. An introduction to statistical communication theory **960** McGraw-Hill New York (1960).

115. Waring, G. T., Nttestad, L., Olsen, E., Skov, H. & Vikingsson, G. Distribution and density estimates of cetaceans along the mid-Atlantic Ridge during summer 2004. *J. Cetacean Res. Manage* **10**, 137-146 (2008).

116. Forney, K. A. & Barlow, J. Seasonal patterns in the abundance and distribution of California cetaceans, 1991–1992. *Marine Mammal Sci.* **14**, 460-489 (1998).

117. Kane, J. Decadal distribution and abundance trends for the late stage copepodites of *Pseudocalanus* spp. (Copepoda: Calanoida) in the US Northeast continental shelf ecosystem. *J. Northw. Atl. Fish. Sci.* **46** 1-13 (2014).

118. Kane, J. A comparison of two zooplankton time series data collected in the Gulf of Maine. *J. of Plankton Research*, **31**, 249-259 (2009).

119. Kane, J. & Prezioso J. Distribution and multi-annual abundance trends of the copepod Temora longicornis in the US Northeast Shelf Ecosystem. *J. of Plankton Research*, **30**, 619-632 (2008).

120. Kane, J. Zooplankton abundance trends on Georges Bank, 1977-2004. *ICES J. of Marine Science: Journal du Conseil*, **64**, 909-919 (2007).

121. Beardsley, R. C. *et al.* Spatial variability in zooplankton abundance near feeding right whales in the Great South Channel. *Deep Sea Research Part II: Topical Studies in Oceanography* **43**, 1601-1625 (1996).

122. Watkins, W. A. & Schevill, W. E. Aerial observation of feeding behavior in four baleen whales: *Eubalaena glacialis, Balaenoptera borealis, Megaptera novangliae,* and *Balaenoptera physalus. J. of Mammalogy*, **60**, 155-163 (1979).

123. Friedlaender, A. S. *et al.* Whale distribution in relation to prey abundance and oceanographic processes in shelf waters of the Western Antarctic Peninsula. *Mar. Ecol. Prog. Ser.* **317**, 297-310 (2006).

124. Schoenherr, J. R. Blue whales feeding on high concentrations of euphausiids around Monterey Submarine Canyon. *Canadian J. of Zoology*, **69**, 583-594 (1991).